



Cite this: *Chem. Soc. Rev.*, 2015,
44, 7715

Electronic transport properties of transition metal dichalcogenide field-effect devices: surface and interface effects

Hennrik Schmidt,^{†,ab} Francesco Giustiniano^{†,ab} and Goki Eda^{*abc}

Recent explosion of interest in two-dimensional (2D) materials research has led to extensive exploration of physical and chemical phenomena unique to this new class of materials and their technological potential. Atomically thin layers of group 6 transition metal dichalcogenides (TMDs) such as MoS₂ and WSe₂ are remarkably stable semiconductors that allow highly efficient electrostatic control due to their 2D nature. Field effect transistors (FETs) based on 2D TMDs are basic building blocks for novel electronic and chemical sensing applications. Here, we review the state-of-the-art of TMD-based FETs and summarize the current understanding of interface and surface effects that play a major role in these systems. We discuss how controlled doping is key to tailoring the electrical response of these materials and realizing high performance devices. The first part of this review focuses on some fundamental features of gate-modulated charge transport in 2D TMDs. We critically evaluate the role of surfaces and interfaces based on the data reported in the literature and explain the observed discrepancies between the experimental and theoretical values of carrier mobility. The second part introduces various non-covalent strategies for achieving desired doping in these systems. Gas sensors based on charge transfer doping and electrostatic stabilization are introduced to highlight progress in this direction. We conclude the review with an outlook on the realization of tailored TMD-based field-effect devices through surface and interface chemistry.

Received 1st April 2015

DOI: 10.1039/c5cs00275c

www.rsc.org/chemsocrev

1. Introduction

Two-dimensional (2D) materials offer an exciting platform for basic research as well as prospects for technological breakthroughs in a number of applications. Since the observation of unusual physical properties of graphene triggered an explosion of research in 2004,^{1,2} a wide variety of 2D materials such as MoS₂^{3,4} and black phosphorus⁵ have also received increasing attention, particularly in the last couple of years. The diversity of materials that exist in van der Waals layer structure offers an unlimited catalogue of 2D materials with a range of intriguing properties as discussed in recent reviews.^{6–10} These emerging 2D materials and their heterostructures offer tremendous opportunities in the exploration of fundamental condensed matter phenomena as well as realization of novel technologies.¹¹

The past few years have seen rapid development of 2D materials research focusing on the family of transition metal dichalcogenides (TMDs). Most notably, exploration of group 6 TMDs such as MoS₂ and WSe₂, which are stable semiconducting compounds with a band gap in the visible to near infrared (NIR) frequencies, revealed their remarkable features such as excellent electrostatic coupling,¹² layer-dependent tunable bandgaps,¹³ direct-to-indirect bandgap crossover,¹³ gate tunable superconductivity,¹⁴ photo-switching,¹⁵ and valley-selective optical excitation^{16,17} to name a few. While the carrier mobility of 2D TMDs is modest compared to graphene due to the high effective mass of the carriers, the unique set of properties displayed by this group of materials make them potentially useful for field-effect transistors (FETs),¹⁸ light harvesting devices,¹⁹ ultrasensitive chemical sensors,^{20–22} flexible electronics^{23,24} and spintronics.¹⁶

Charge transport properties of bulk TMD crystals have been extensively studied since the early work by Fivaz and Mooser.²⁵ However, detailed electrical characterization of 2D crystals was hampered by the small size of the samples that could be obtained by mechanical²⁶ and chemical^{27,28} exfoliation. FETs from bulk²⁹ and few-layer³⁰ TMD crystals were demonstrated more recently followed by the pioneering work on monolayer

^a Graphene Research Centre, National University of Singapore, 6 Science Drive 2, Singapore 117546

^b Department of Physics, National University of Singapore, 2 Science Drive 3, Singapore 117542

^c Department of Chemistry, National University of Singapore, 3 Science Drive 3, Singapore 117543. E-mail: g.eda@nus.edu.sg

† These authors contributed equally to this work.

MoS_2 FETs¹² and logic gates³¹ by Kis's group. Mono- and few-layer FETs from the isoelectronic compounds of MoS_2 such as MoSe_2 ,^{32–34} WSe_2 ,^{35,36} WS_2 ,^{37–39} and MoTe_2 ^{40,41} have also been successfully demonstrated.

Group 6 TMDs are stable under ambient conditions, compared to semiconducting TMDs from other groups such as TiS_2 ⁴² and other semiconducting 2D materials such as phosphorene,^{43,44} which is known to oxidize over time.⁴⁵ Nevertheless, the electrical properties of 2D MX₂ devices (M = Mo and W; X = S and Se) are known to be highly sensitive to extrinsic effects that arise from surfaces and interfaces such as metal contacts, surface adsorption, dielectric interfaces, and surface defects. While sensitivity to environmental factors offers opportunities for novel sensing applications, unintentional extrinsic effects often obscure the intrinsic electrical response of the material. This is evident from



Hennrik Schmidt

Dr Hennrik Schmidt received his PhD in 2012 at the Leibniz University in Hannover, Germany. Afterwards, he worked as a research fellow at the Centre for Advanced 2D Materials and Graphene Research Centre at the National University of Singapore from 2013 to 2015. The main focus of his research lies on the experimental characterization of electronic and thermoelectrical properties as well as low temperature quantum transport of atomically thin crystals. His previous works include studies on graphene, especially its twisted bilayers, transition metal dichalcogenides, and black phosphorous.



Francesco Giustiniano

inorganic materials for nanoelectronic applications (molecular wires, nanoparticles, and transition metal dichalcogenide single crystals) with a focus on the self-assembly of conductive thin films, high-throughput electrical testing, sensor development and graphene processing.

the notable gap between the theoretically predicted behaviours of MX₂ and experimental observations. In fact, there is also a significant disparity in the experimentally reported values of device performance parameters such as carrier mobility. Thus, in order to identify opportunities and challenges for the realization of 2D TMD-based devices, it is crucial to develop a comprehensive understanding of the role of surfaces and interfaces and to establish strategies for tailoring them to achieve the desired device performance and functionalities.

Here, we review recent developments in the understanding of interface and surface effects in the electronic devices based on group 6 TMD 2D crystals. In the first part, we will start by introducing basic materials properties and device operation principles. We will discuss how gate-modulated charge transport offers insights into the role of chemical environments. This will be followed by a summary of various strategies used to improve the performance of FETs. Some fundamental aspects of charge transport will be discussed to highlight the importance of doping. In the second part, we will introduce various techniques for achieving desired doping in these materials. We will conclude the review with an outlook for device optimization strategies and sensing applications of TMD-based FETs.

2. Atomic and electronic structure

The basic properties of TMD crystals have been studied for over half a century (see ref. 46 for a comprehensive review of early studies). An individual TMD monolayer consists of an X-M-X sandwich (Fig. 1a) with primarily covalent intra-layer bonding. Despite their structural similarity, layered TMDs display a wide range of electrical properties depending on the number of electrons in their non-bonding d orbitals and the coordination geometry of the metal atom (see ref. 47 and 48 for a discussion of the crystal structure, the band structure and optical properties).



Goki Eda

Dr Goki Eda received his MSc in Materials Science and Engineering from Worcester Polytechnic Institute in 2006 and PhD in the same discipline from Rutgers University in 2009. He became a Newton International Fellow of the Royal Society of UK and worked at Imperial College London. Dr Eda joined the National University of Singapore as an Assistant Professor of Physics and Chemistry in 2011. He is a recipient of the Singapore National Research Foundation (NRF) Research Fellowship and a member of the Centre for Advanced 2D Materials. His research interest includes light-matter interaction and charge transport in 2D crystals.

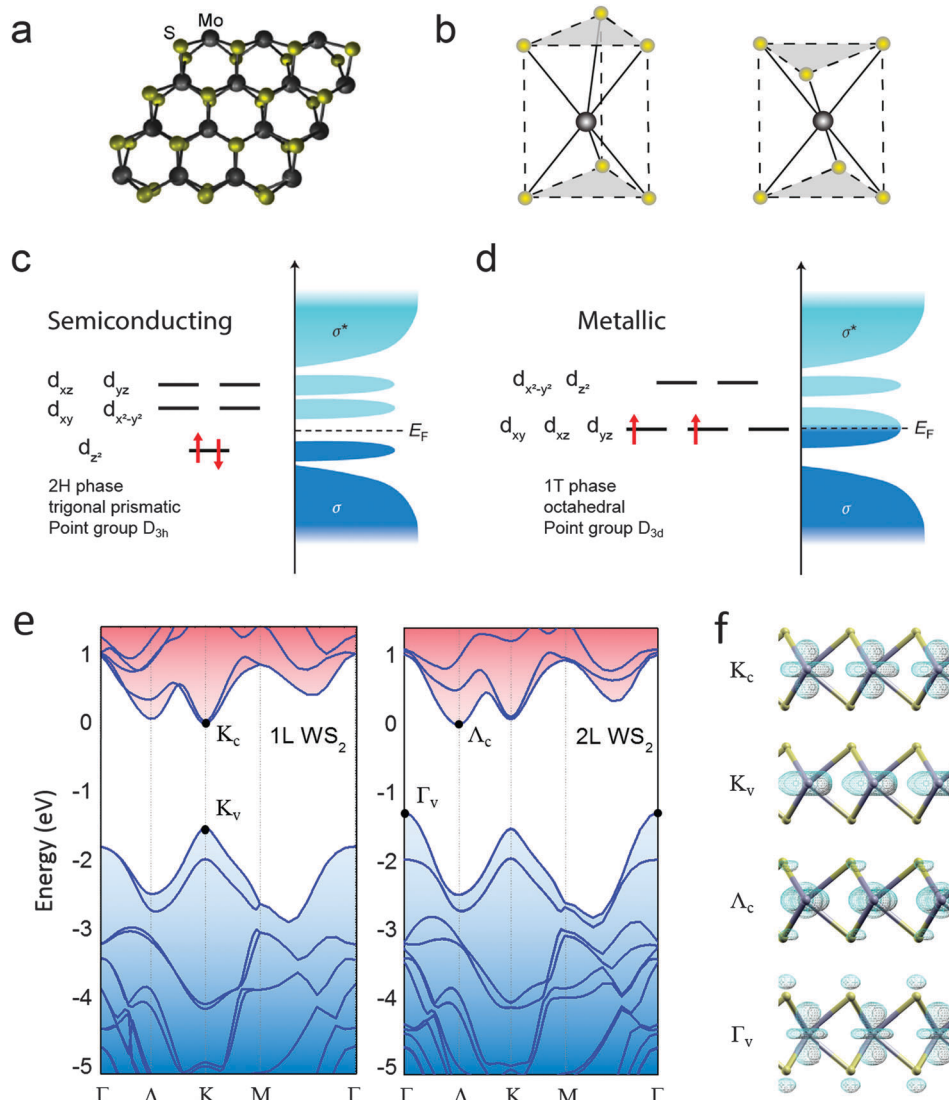


Fig. 1 Atomic and electronic structure. (a) Top view of a monolayer MoS₂ structure. (b) Schematics of the trigonal prismatic (left) and octahedral (right) coordination geometries. (c and d) Filling of the non-bonding d-orbitals for a typical d² TMD along with the band structure and the representative position of the Fermi level for (c) 2H phase and (d) 1T phase. (e) Calculated electronic band structure of mono- (left) and bilayer (right) WS₂. The dots indicate the valence band maximum (VBM) and the conduction band minimum (CBM). (f) Representative isosurface plot for states associated with different parts of the band structure. Notice the change in electrical properties due to the different band structure in the two phases. (a) Reprinted with permission from ref. 50. Copyright 2013 American Chemical Society. (c and d) Reprinted with permission from ref. 51. Copyright 2013 Nature Publishing Group. (e) Courtesy of Prof. Ricardo Mendes Ribeiro. (f) Reprinted with permission from ref. 52. Copyright 2015 American Chemical Society.

Group 6 TMDs such as MoS₂ and WSe₂ are semiconductors with an optical bandgap in the range of 1–2 eV depending on the number of layers. Layered TMDs often occur in different polymorphs (metal coordination geometry) and polytypes (stacking order). It is possible to produce mm- to cm-size TMD crystals with a particular structure by controlling the growth parameters.⁴⁹ The materials are usually named by following the stacking order, and polytypes such as 2H (2-layer unit cell, hexagonal), 3R (3-layer unit cell, rhombohedral), and 1T (1-layer unit cell, trigonal) are common. Note that the geometry implied in this naming scheme refers only to the vertical arrangement of the layers in the basic unit cell and not to the geometry of the metal coordination (polymorphism). Strictly speaking, these nomenclatures are not

fully applicable to single layer MX₂ (a 2H-MX₂ monolayer simply means a monolayer isolated from a 2H bulk material).

Polymorphism or metal coordination can have a significant influence on the electronic properties of TMDs. For example, MoS₂ in trigonal prismatic coordination is semiconducting whereas its octahedral phase is metallic (Fig. 1b–d). From a ligand field theory perspective, the semiconducting nature of trigonal prismatic MoS₂ is due to the completely filled d_{z2} and empty d_{xy} and d_{x²-y²} orbitals (Fig. 1c). Octahedral MoS₂ is metallic because of its partially filled t_{2g} band (d_{xy}, d_{xz}, d_{yz}).

Another key aspect of group 6 TMDs is the effect the number of layers has on the electronic band structure. While monolayers are direct gap semiconductors, multilayer materials display

an indirect band gap as a result of interlayer orbital interactions. That is, due to the higher p-character at the Γ_v (v: valence) and Λ_c (c: conduction) points of the band structure, interlayer interaction results in higher and lower energies, respectively, at these points compared to the monolayer case, and an indirect band gap is formed in multilayers. The states at the K points, or the corners of the Brillouin zone are only marginally affected by the neighbouring layers due to their pronounced d-character and localization of the charges in the middle of the X–M–X structure (Fig. 1e and f). In this review, we will focus mainly on mono- and few-layer 2H-MX₂, which is the thermodynamically stable phase with trigonal prismatic coordination. The possibility to access 1T-MoS₂ is also briefly discussed.

3. Materials

Mono- and few-layer TMDs can be readily obtained by the well-known mechanical exfoliation of bulk crystals.² 2D crystals with lateral sizes of up to tens of micrometers can be prepared using this technique (Fig. 2a). The number of layers can be estimated

from optical contrast and more precisely determined by atomic force microscopy (AFM). Raman (Fig. 2e) and photoluminescence (PL) spectroscopy (Fig. 2f and g) also offer information on the number of layers, as well as on doping and strain levels.^{53–57}

Other methods to obtain monolayers include solution-based exfoliation techniques,^{8,58} post-deposition etching (chemical,^{59,60} plasma⁶¹ and photothermal⁶²), chemical synthesis,⁶³ and atomic layer deposition.⁶⁴ Solution-based techniques typically yield colloidal suspensions of submicron-sized nanosheets. Note that the starting bulk crystals can be obtained either from natural sources or synthesized by techniques such as chemical vapour transport (CVT).⁶⁵ Chemical vapor deposition (CVD) of monolayers onto amorphous SiO₂, quartz, and sapphire substrates has been demonstrated by many groups for MoS₂,^{66–81} MoSe₂,^{32,82} WS₂⁸³ and WSe₂.^{84,85} Alloys such as MoS_xSe_{2-x}⁸⁶ and doped TMDs⁸⁷ can also be prepared by either the CVD or CVT technique. CVD-grown samples are polycrystalline with grains having sizes of tens of nanometers to tens of micrometers. While charge transport studies^{70,78} have indicated that grain boundaries perpendicular to the current flow have detrimental effects on carrier mobility, individual crystallites of CVD-grown

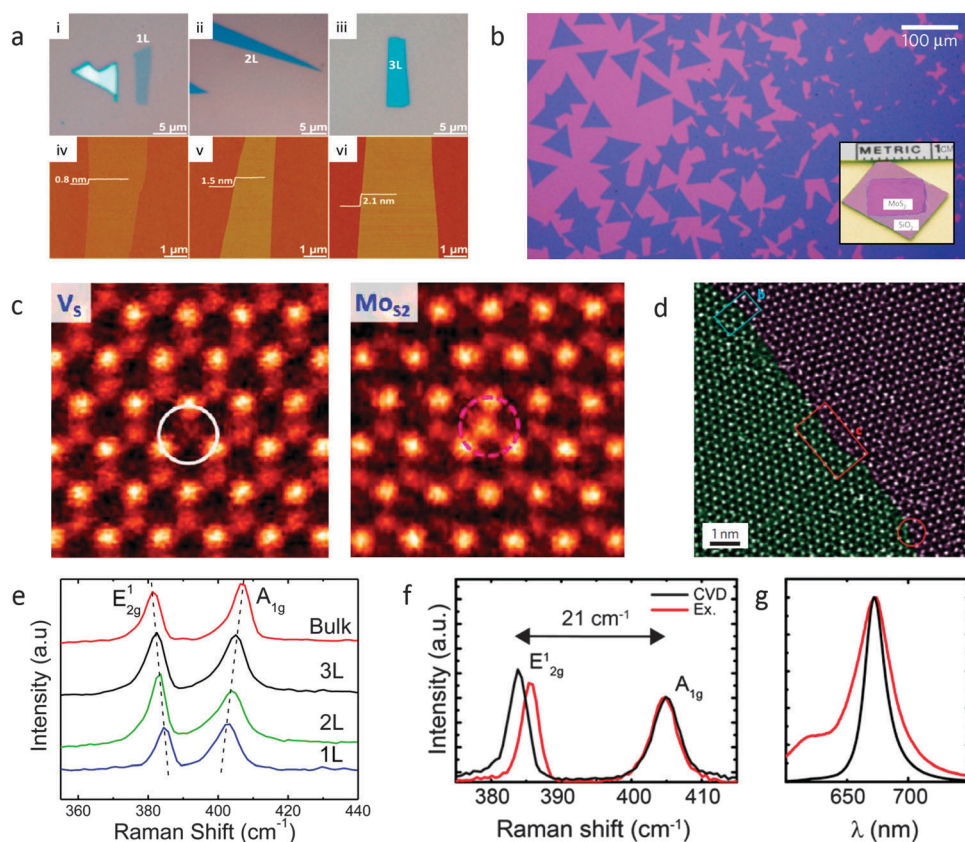


Fig. 2 Material structure and characterization. (a) Optical and AFM images of mono-, bi-, and trilayer MoS₂. (b) Optical image of large-area monolayer MoS₂ grown by CVD on the Si/SiO₂ substrate. The inset shows the sample size. (c) High resolution dark-field STEM image of mechanically exfoliated MoS₂ showing sulfur vacancy (left) and antisite substitution (right). (d) STM image of a grain boundary in CVD MoS₂. (e) Evolution of Raman spectra with increasing number of layers. (f and g) Comparison of exfoliated and CVD MoS₂ monolayers by (f) Raman and (g) PL spectroscopy. (a) Reprinted with permission from ref. 100. Copyright 2014 American Chemical Society. (b) and the inset reprinted with permissions from ref. 70 and 72. Copyright 2013 Nature Publishing Group. (c) Reprinted with permission from ref. 90. Copyright 2014 American Chemical Society. (d) Reprinted with permission from ref. 72. Copyright 2014 Nature Publishing Group. (e) Reprinted with permission from ref. 101. Copyright 2011 American Chemical Society. (f and g) Reprinted with permission from ref. 79. Copyright 2014 American Chemical Society.

materials can be of high electronic quality comparable to or superior to those of mechanically exfoliated counterparts.⁷⁹ It is worth noting that initial attempts to fabricate transistor arrays for wafer-scale electronic circuits have shown promising results.^{71,88}

Recent studies have shown that sulfur vacancies and antisite substitutions (S replaced by Mo) are the most commonly occurring point defects in MoS₂.^{89,90} It has been suggested that such point defects play a major role in the electronic properties and device behaviours of TMDs.⁹¹ For bulk MoS₂, n-type doping has been attributed to donor states arising from sulfur vacancies.⁹² It is believed that vacancy defects also play a role⁹³ in the observed strong n-type doping of monolayer MoS₂.^{12,50,79,94} The reported sulfur vacancy densities vary from $3.5 \times 10^{10} \text{ cm}^{-2}$ in bulk MoS₂ samples⁹² as measured by scanning tunneling microscopy (STM) to significantly higher values of the order of 10^{13} cm^{-2} for monolayer MoS₂^{95,96} as measured by scanning transmission electron microscopy (STEM). A method for ‘healing’ the sulfur vacancies *via* thiol wet chemistry has been recently developed by Makarova *et al.*⁹⁷ Another report shows that the density of vacancies can be reduced by 75% when this technique is used to treat both sides of monolayer MoS₂.⁹⁶

Preparation of multilayer MX₂ with deliberately introduced stacking disorder have been reported.⁹⁸ These twisted multilayers exhibit distinct electronic structure due to reduced coupling of the layers.⁹⁹ Control of stacking order is a viable route for engineering the band gap of these materials.

4. Device structure

The change in electrical conductivity or resistivity as a function of charge carrier density provides rich information on the electronic properties of a material. Carrier mobility μ , which is often used as a figure of merit for the electronic quality or switching speed of semiconductor devices, is defined as

conductivity σ per unit charge or $\mu = \sigma/en$ where n is the density of charge carriers and e is the elementary charge. Since carrier density is often not precisely known, many studies quote field effect mobility μ_{FE} , which is an effective approximation of mobility extracted from a transfer curve *i.e.* a plot of σ vs. gate voltage V_G . Assuming that the charge carrier density changes linearly with the gate voltage, $\mu_{\text{FE}} = 1/C \times d\sigma/dV_G$ where C is the capacitance of the gate dielectric. It is worth noting that field effect mobility tends to overestimate the actual carrier mobility according to a recent study.⁵⁰ Intrinsic carrier mobility and field effect mobility should in principle coincide in the linear regime of the transfer curve.

The carrier density of a semiconductor can be systematically modulated by electrostatic or electrochemical gating in a FET configuration. In a simple case, two metal electrodes (source (S) and drain (D)) deposited on the sample are used to monitor its conductivity while the third electrode (gate (G)) induces either negative or positive charges on the sample surface across a gate dielectric material. This configuration yields a reasonable measure of carrier mobility as long as the contact resistance is significantly lower than the channel resistance. However, this is often not the case and a more accurate measurement technique is needed. The channel conductivity can be more precisely measured without the influence of contact resistance in four-terminal geometry where the outer probes are used as a current source and a drain, and the inner probes are used to monitor the resulting voltage drop. Furthermore, for the precise measurements of carrier density, the Hall effect can be measured.^{50,102} This requires simultaneous measurements of the longitudinal (V_{xx}) and transverse (V_{xy}) voltages with properly designed electrodes (Fig. 3a and b).

The most commonly used gate geometry is global back-gating, where the heavily doped silicon substrate and thermal oxide are used as the back gate electrode and the dielectric layer, respectively. In this simple configuration, the charge

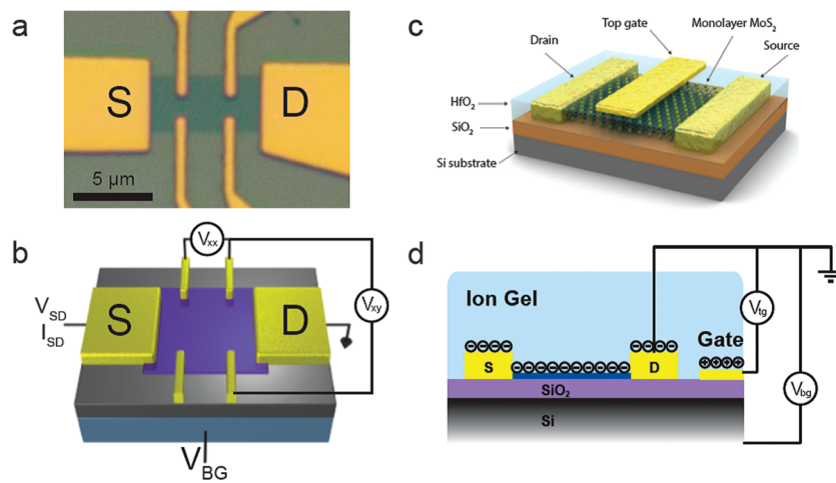


Fig. 3 Device structures. (a) Optical microscopy image of a typical field effect device. (b) Schematic of a backgated multiterminal device. V_{SD} and I_{SD} are the voltage and current between the source (S) and drain (D) electrodes; V_{BG} is the backgate voltage used to electrostatically gate the channel. (c) Schematic of a device with a solid top gate dielectric (HfO₂). (d) Schematic of a dual gated device with the ionic gel top gate and the Si back gate. (b) Reprinted with permission from ref. 50. Copyright 2013 American Chemical Society. (c) Reprinted with permission from ref. 12. Copyright 2011 Nature Publishing Group.

carrier density in the sample above the threshold voltage V_{th} can be estimated by $n = \alpha(V_{\text{BG}} - V_{\text{th}})$, where V_{BG} is the backgate voltage and α is a constant unique to the dielectric material and its thickness (*e.g.* for 300 nm SiO₂, the gate capacitance is $C_{\text{ox}} = 11.5 \text{ nF cm}^{-2}$, and $\alpha = C_{\text{ox}}/e = 7.2 \times 10^{10} \text{ cm}^{-2} \text{ V}^{-1}$). The semiconducting channel can also be gated *via* a top gate dielectric.¹² Commonly used dielectric materials are Al₂O₃ and HfO₂ layers deposited by atomic layer deposition (ALD) (Fig. 3c). Extraction of device parameters in top-gated FETs requires extra care for the estimation of gate capacitance as discussed by Fuhrer and Hone.¹⁰³

Solid gate dielectrics typically allow modulation of carrier densities up to 10^{13} cm^{-2} . Larger modulation of carrier densities can be achieved by ionic or electrochemical gating *via* formation of an electric double layer (EDL).^{104,105} In this case, electrolyte solution or ionic liquid is directly applied to the channel region. When a bias is applied between the sample and the gate electrode immersed in the electrolyte solution or ionic liquid, ions migrate to the channel surface and form an EDL (Fig. 3d). Since the EDL thickness is typically 1 nm or less, it exhibits extremely large capacitance and induces high carrier density ($>10^{13} \text{ cm}^{-2}$) at small gate biases (typically $<5 \text{ V}$). Ionic gating offers a versatile route for realizing flexible FET devices on plastic substrates and formation of lateral p-n junctions.¹⁰⁶ Its high capacitance also allows modulation of the chemical potential of semiconductors over a wider range of energies, often allowing access to both the conduction and valence bands, which is often challenging with solid dielectrics for semiconductors with a sizeable band gap ($\sim 2 \text{ eV}$).^{107–109} Drawbacks of ionic gating include the slow response time and often limited electrochemical stability windows. An ionic top gate can be used in combination with the SiO₂ back

gate to achieve precise modulation of charge carrier densities over a wide range and electric fields as demonstrated previously for graphene^{110–112} and more recently for MoS₂.^{14,23,109}

5. Device characteristics

Typical transfer curves for monolayer WSe₂ and MoS₂ FET devices are shown in Fig. 4a and b, respectively. WSe₂ is conducting at negative gate biases and becomes insulating at positive gate biases, indicating that it is a p-type semiconductor. In contrast, MoS₂ shows an opposite gate dependence, turning “on” at positive gate biases, displaying its n-type character. The conductivity typically reaches several hundreds of micro-siemens (μS) (or several kilo-ohms ($\text{k}\Omega$) in resistivity) when the device is in the on-state.

At low carrier densities (*i.e.* small gate voltages), the temperature dependence is insulator-like and the conductivity increases with increasing temperature. On the other hand, a metallic behavior (*i.e.* conductivity decreases with increasing temperature) is observed in the high carrier density and high conductivity regime. Studies^{50,113,114} have shown that this cross-over, sometimes referred to as the metal-insulator transition (MIT), occurs at conductivities of around e^2/h (38.7 μS).

The transfer curve of ionically gated devices often shows both electron and hole branches independent of the inherent polarity of the material (Fig. 4c). Gating is particularly effective for ultrathin samples (1–2 layers) due to minimal screening of the electric field as it can be seen from the large on-off ratio (the ratio of current in the on and off states). Bulk flake devices

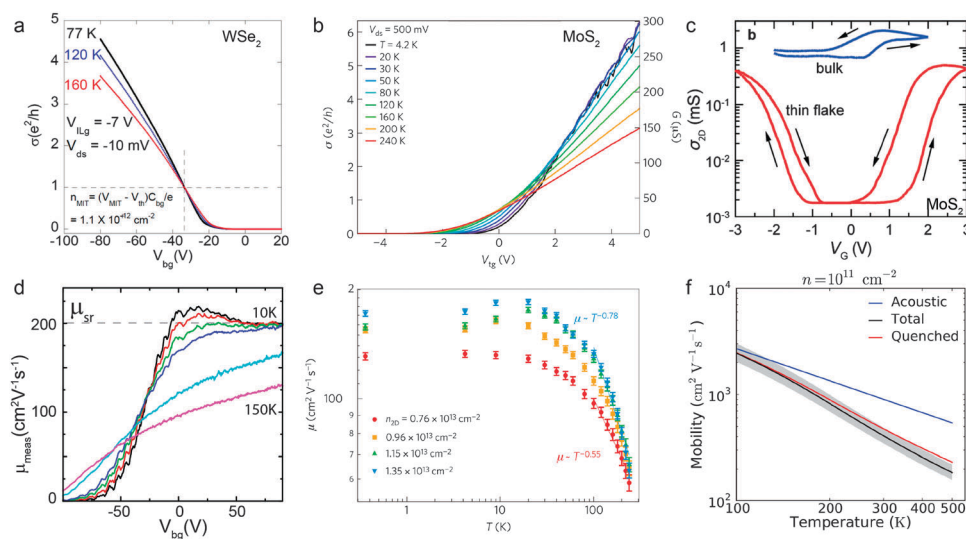


Fig. 4 Device characteristics. (a and b) Electrical conductivity of monolayer (a) WSe₂ and (b) MoS₂ as a function of gate voltage. (c) Transfer curves of ionically gated FETs with thin and thick MoS₂ flakes. (d) Field-effect mobility of monolayer MoS₂ as a function of gate voltage showing saturation at low temperatures. (e) Carrier mobility of MoS₂ as a function of temperature for different carrier densities. (f) Theoretically predicted phonon-limited carrier mobility of MoS₂ above 100 K. (a) Reprinted with permission from ref. 114. Copyright 2014 American Chemical Society. (b and e) Reprinted with permission from ref. 113. Copyright 2013 Nature Publishing Group. (c) Reprinted with permission from ref. 108. Copyright 2012 American Chemical Society. (d) Reprinted with permission from ref. 79. Copyright 2014 American Chemical Society. (f) Reprinted figure with permission from ref. 116. Copyright 2012 by the American Physical Society.

typically show higher conductance but low on-off ratios compared to monolayer devices due to screening effects.^{94,115}

At low temperatures and at high gate voltages, the transfer curves often become linear, indicating the saturation of field effect mobility (Fig. 4d). In the non-linear regime, field effect mobility increases gradually with gate voltage, indicating changes in the conduction mechanism. Saturation of mobility is also reached with decreasing temperature for devices in the metallic conduction regime as shown in Fig. 4e. This temperature dependence has been consistently observed in most of the MX_2 devices reported to date.

Calculations by Kaasbjerg *et al.*^{116,117} show that the mobility of MoS_2 at room temperature is predominantly limited by phonon scattering. The calculated phonon-limited mobility increases with decreasing temperature as $T^{-\gamma}$, where γ is the phonon damping factor of the order of 1–2, and it reaches several thousand $\text{cm}^2 \text{V}^{-1} \text{s}^{-1}$ at temperatures below 100 K (Fig. 4f).¹¹⁷ In contrast to the theoretical predictions, most of the experimental studies to date have shown that the mobility remains below $1000 \text{ cm}^2 \text{V}^{-1} \text{s}^{-1}$ and saturates at low temperatures.^{79,118} It is thus evident that phonons are not the limiting factors in this temperature regime. Specifically, short- and long-range scattering from defects and impurities are expected to play a dominant role at low temperatures.

6. Charge transport regimes

The carrier conduction mechanism in 2D MX_2 is strongly dependent on the carrier density or equivalently the Fermi energy E_F as schematically illustrated in Fig. 5. The changes in the conduction mechanism are evident from the temperature dependence of device conductivity or resistivity (Fig. 5a). The insulating state of the device can be represented by E_F lying in the bandgap region and the absence of mobile carriers (Fig. 5b). Positive gate bias shifts E_F to the conduction band edge where electrons start to become mobile with the help of thermal excitation and contribute to conduction (Fig. 5c). A further increase in gate bias leads to the shift of E_F above the mobility edge where band transport occurs (Fig. 5d). Similar discussions can be made for the transport of holes at negative gate biases.

The transition from the insulating state to the conducting state is often gradual, involving progressive filling of the localized states or band edge disorder states arising from impurities and structural defects (Fig. 5e). At intermediate doping levels, electrical conduction occurs *via* localized states, often described by the variable range hopping (VRH) model.^{101,118,119} The conductance in this regime follows $\sigma \sim AT^m \exp(-T_0/T)^{1/(d+1)}$ where d is the dimension in which transport takes place ($d = 2$ for 2D materials) and $m = 0.8$ is an empirical exponent. The resistivity of MX_2 typically varies widely in this conduction regime from 10^5 to $10^{12} \Omega$, decreasing with increasing temperatures. Band transport through extended states is indicated by the change in the sign of the temperature dependence and low device resistance on the order of 10^2 to $10^4 \Omega$. In this regime, the transport is limited by phonons, and

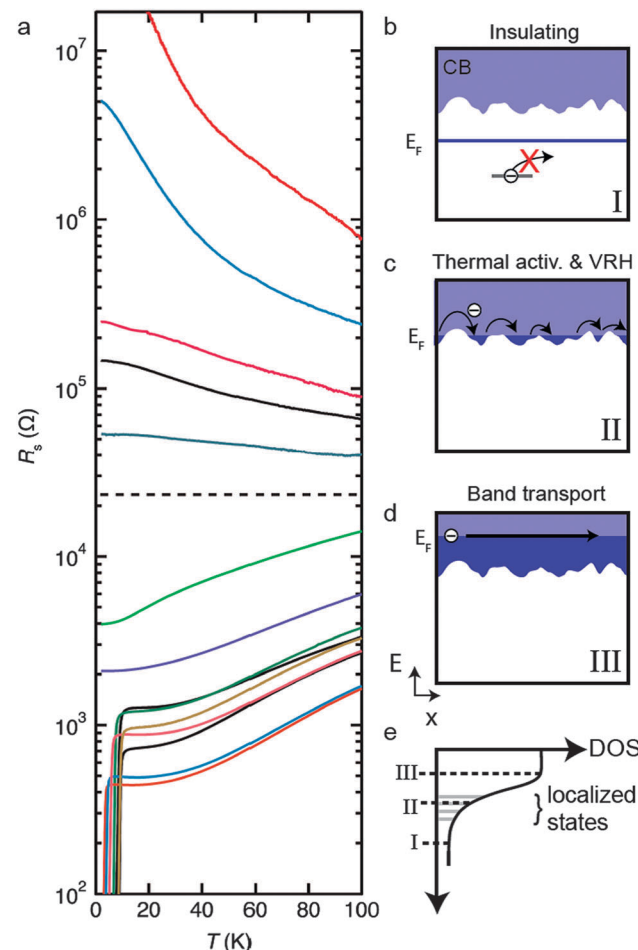


Fig. 5 Charge transport regimes. (a) Temperature dependent resistivity of ionically gated few-layer MoS_2 devices. The temperature dependence evolves significantly from insulating at low carrier densities (top curves) to metallic and superconducting at high carrier densities (bottom curves). (b-d) Schematic energy diagram representing different charge transport regimes: (b) insulating; (c) conducting by thermal activation and by hopping; and (d) band transport. (e) Density of states (DOS) diagram showing the disorder-derived band tail states. (a) Reprinted with permission from ref. 14. Copyright 2012 AAAS.

short- and long-range scatterers such as defects and charged impurities. Band transport can be achieved at sufficiently large doping concentrations (typically $>10^{13} \text{ cm}^{-2}$). Recently it was shown that few-layer MoS_2 becomes superconducting at critical temperatures of up to 10 K when the carrier concentration is increased above $6 \times 10^{14} \text{ cm}^{-2}$.¹⁴

7. Carrier mobility

Fig. 6 summarizes the mobility values of TMD devices reported in the current literature. The data points are sorted by different carrier types, flake thicknesses, substrates, measurement temperatures and other measurement conditions. It is clear that the data points are scattered over a wide range even for measurements conducted under similar conditions. This considerable spread in the data highlights that TMD device performance

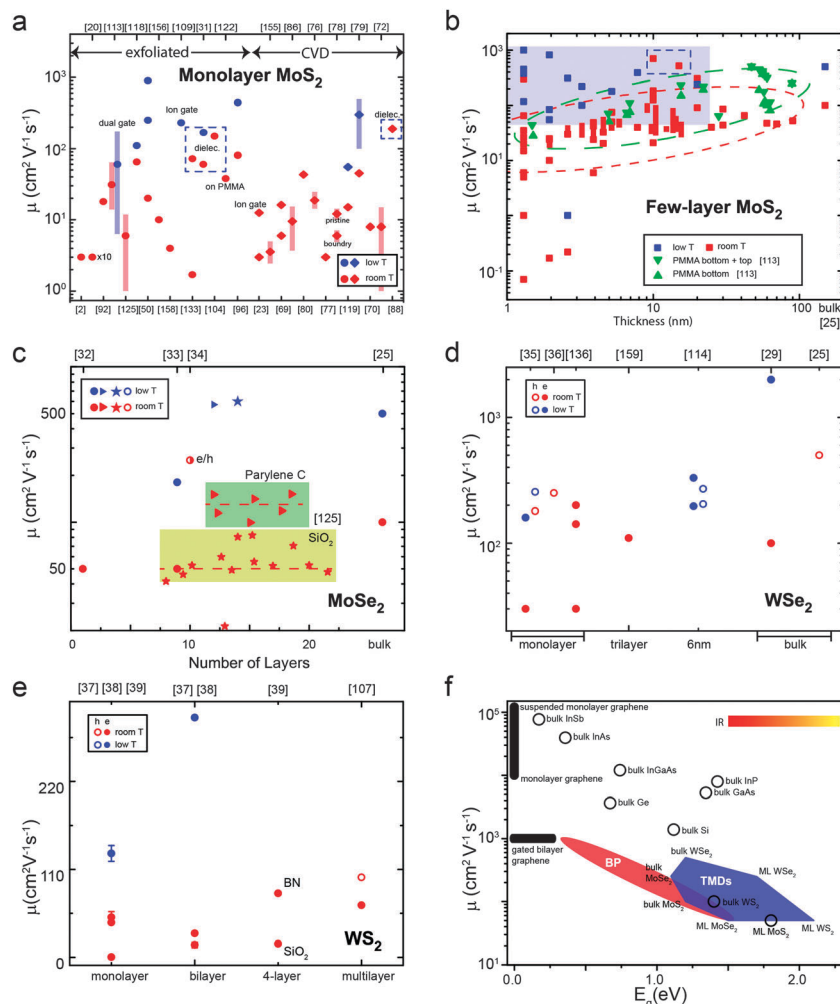


Fig. 6 Carrier mobility. Carrier mobilities reported for (a) monolayer and (b) few-layer MoS₂. (c–e) Mobility values for mono- and few-layer (c) MoSe₂, (d) WSe₂, and (e) WS₂. (f) Plot of mobilities vs. band gap for various semiconductors. The color scale represents the energy range of visible and infrared (IR) light with respect to the band gap energy. The bandgap values of TMDs are optical bandgaps obtained from the review by Wang *et al.*⁵

is sensitively influenced by subtle differences in the material quality, device fabrication procedures, device configuration, and measurement conditions. Nevertheless, some general trends can be identified as discussed below. Note that the values reported here are mostly electron mobilities reflecting the tendency of these materials to be doped by electron donors. Hole conduction has been observed in monolayer WSe₂ and multilayer samples of other materials.

7.1 MoS₂

The electron mobility values of monolayer MoS₂ (Fig. 6a) are widely spread across 3 orders of magnitude ($1\text{--}1000\text{ cm}^2\text{ V}^{-1}\text{ s}^{-1}$). It is clear that the low temperature mobilities are significantly higher than the room temperature values, indicating that phonon scattering is a dominant factor limiting carrier mobility at room temperature. There are no distinctions between the mobility values of mechanically exfoliated and CVD-grown samples. This suggests that the grain boundaries in CVD TMDs have a less dominating influence on charge transport compared to point defects such as sulfur vacancies that are present in each

grain. This behaviour is in contrast to the case of graphene, for which grain boundaries in CVD samples often severely limit the carrier mobility below that of individual grains or mechanically exfoliated samples.¹²⁰ These observations may suggest that the quality of CVD-grown MoS₂ is comparable to that of mechanically exfoliated ones. Alternatively, these results may be explained by the strong contributions of extrinsic factors in masking differences in the intrinsic material properties. The roles of extrinsic factors are discussed in more detail in the following section.

The trend in Fig. 6b shows that the room temperature mobility increases with increasing number of layers. Li *et al.*¹²¹ attributed this effect to the presence of charged impurities on the substrate, which influences thinner samples more strongly. Bao *et al.*¹²² showed that devices on polymethylmethacrylate (PMMA)-coated substrate exhibit improved carrier mobilities (solid upright and inverted triangles), indicating that the detrimental effects arising from the SiO₂ substrate can be alleviated. The authors also showed that the mobility can be further improved by encapsulating the channel with PMMA and proposed that

charged impurity scattering dominates in these devices. Similar effects were observed on hexagonal boron nitride (hBN) substrates.¹²³ The hole mobility of multilayer MoS₂ was found to be comparable to the electron mobility, indicating that the effective masses of the carriers are similar to those predicted by the calculations.¹²⁴

7.2 MoSe₂, WSe₂, and WS₂

Fig. 6c, d and e summarize available mobility data of MoSe₂, WSe₂ and WS₂ from the literature. Typical mobility values lie between 1 and 1000 cm² V⁻¹ s⁻¹. The hole mobilities are typically comparable to or slightly larger than the electron mobility. The general behaviours of these materials are similar to those of MoS₂. Chamlagain *et al.*¹²⁵ observed that MoSe₂ exhibits enhanced mobility when deposited on polyimide C-coated SiO₂ instead of bare SiO₂, similar to the effect of PMMA on MoS₂ discussed above.¹²² The use of hBN as the substrate was also shown to yield enhanced mobility for WS₂.³⁹

Fig. 6f summarizes the trends between the carrier mobility and the band gap of MX₂ materials along with representative

semiconductors and other 2D materials such as graphene and black phosphorus. Semiconducting TMDs exhibit lower mobilities compared to conventional bulk semiconductors with a similar band gap such as InP and GaAs. This may be attributed to the heavy effective mass of carriers in TMDs. Black phosphorus has a smaller bandgap (0.3 to 1.5 eV for bulk to few-layer samples)¹²⁶ and exhibits ambipolar transport with balanced electron and hole mobilities in the range of 10–1000 cm² V⁻¹ s⁻¹ in its multilayer form.⁴⁵

8. Extrinsic effects

As the significant spread in mobility values indicates, strategies for optimizing the device performance have not yet been established. There has been increasing evidence that the limiting factors are often not the intrinsic properties of the material. Specifically, the conditions of surfaces and interfaces of a device strongly limit the transport of charges across the 2D TMD layer (Fig. 7a). Below we discuss how surfaces and interfaces may be optimized to tailor device characteristics.

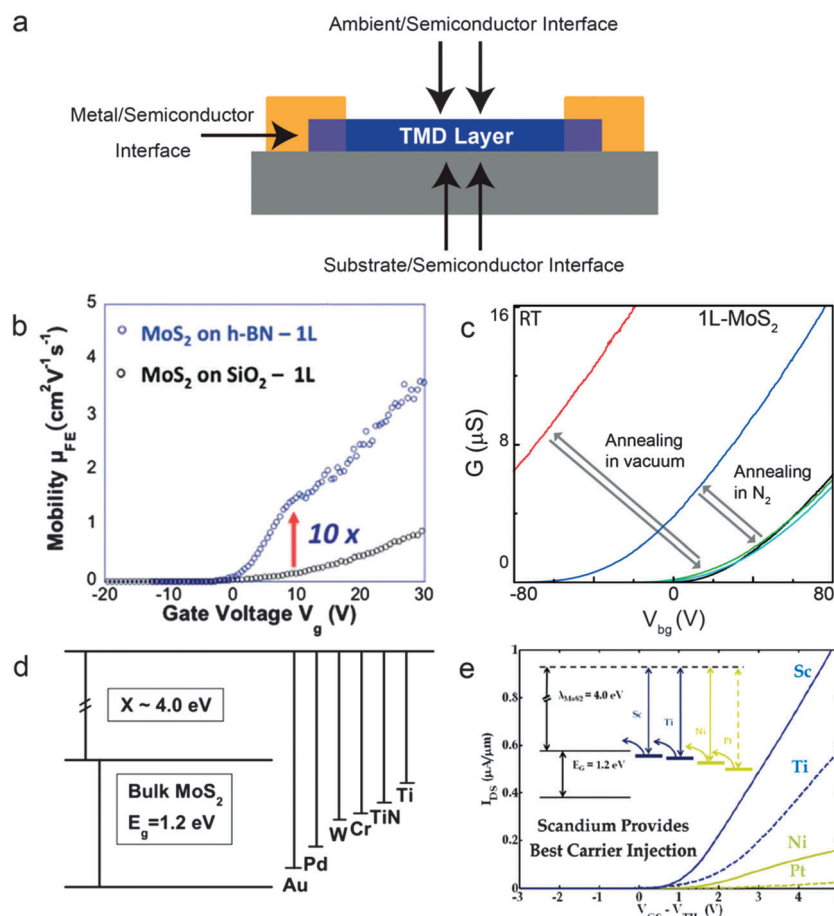


Fig. 7 Extrinsic Effects. (a) Schematic showing the surfaces and interfaces of a TMD FET. (b) Transfer curve of monolayer MoS₂ with and without hBN spacer layers. (c) Transfer curve of monolayer MoS₂ FET before and after vacuum annealing and exposure to air. (d) Schematic showing the conduction and valence band energy levels of bulk MoS₂ and Fermi levels of various metals. (e) Transfer curve of MoS₂ devices having different electrode metals. (b) Reproduced from ref. 127 with permission from The Royal Society of Chemistry. (c) Reprinted with permission from ref. 79. Copyright 2014 American Chemical Society. (d) Reprinted with permission from ref. 91. Copyright 2014 American Chemical Society. (e) Reprinted with permission from ref. 128. Copyright 2013 American Chemical Society.

8.1 Substrate

It is well established that charge transport in graphene is strongly limited by charged impurities,¹²⁹ remote interfacial phonons,¹³⁰ and surface roughness¹³¹ of the substrate. These factors are expected to play an equally important role in TMD devices. The detrimental effects of the substrate may be alleviated in several ways. For example, charged impurities arising from dangling bonds on the substrate surface can be partially passivated by surface functionalization. Alternatively, sandwiching the MX₂ channel with hBN layers can also reduce scattering from charged impurities and roughness.¹³² Fig. 7b shows an example of mobility enhancement enabled by the hBN substrate.^{39,123,127}

8.2 Surface adsorbates

Adsorption of molecular species such as oxygen and water on the surface of MX₂ can significantly alter the doping level and carrier mobility. Fig. 7c shows the transfer characteristics of monolayer MoS₂ before and after mild annealing in vacuum and in N₂ atmosphere. Annealing causes the transfer curve to horizontally shift towards the negative gate voltages, indicating a significant increase in electron doping. This is in fact due to a significant decrease in hole doping due to the removal of electron withdrawing surface adsorbates. Upon exposure of the device to air, the original state is recovered, highlighting the reversible nature of the adsorption process. Because the doping level dictates the transport regime as discussed above, achievable carrier mobility is influenced by surface adsorption. Adsorbed water molecules can also rearrange under an applied electric field, leading to considerable hysteresis in the transfer characteristics.¹³³ Encapsulating the channel with a stable dielectric layer such as PMMA and hBN can partially prevent the molecular species in the gas phase from influencing the device performance.

8.3 Metal-semiconductor junction

MX₂ layers typically form Schottky junctions with the electrode metal. The Schottky barrier, which is undesirable for achieving high performance devices, often contributes a significant portion of the device resistance in MX₂ FETs. The resulting contact resistance is modulated by the gate bias.¹³⁴ Thus, the device operation depends crucially on the choice of the electrode material and the quality of the interface it makes with MX₂. Studies have shown that the Schottky barrier does not solely depend on the work function of the metal (Fig. 7d) but also on the chemical interaction between the metal and MX₂.⁹¹ The electrode metal may alter the electronic properties of the channel material underneath, making it more resistive.¹³⁵

Low work function metals such as scandium and indium have been found to yield low resistance ohmic contacts on multilayer MoS₂¹²⁸ and WSe₂,¹³⁶ respectively (Fig. 7e). Other studies, however, show that high work function metals such as gold also form a low resistance contact with MoS₂,¹² suggesting that Fermi level pinning occurs with some metals.¹³⁷ Low resistance contacts can also be achieved by heavily doping MX₂ in the contact region. Chuang *et al.*¹¹⁴ showed that WSe₂ devices

with heavily doped contacts exhibit significantly improved performance due to a reduced barrier to carrier injection.

The ability to control the spatial distribution, degree, and the polarity of doping is crucial in solving some of the key issues in device optimization. In the following section, we introduce doping strategies for semiconducting MX₂ and discuss how they help in enhancing the device performance and opening up avenues for novel applications.

9. Charge transfer doping

Doping in traditional bulk semiconductors is achieved by introducing substitutional impurities with a valency different from that of the host material. These impurities can be introduced in a controllable manner during or after the growth of the semiconductor. Ion implantation is a versatile technique to achieve spatially controlled incorporation of donor or acceptor impurities.¹³⁸ For group 6 TMDs, group 5 elements such as niobium and group 7 elements such as rhenium can be substitutionally incorporated into the crystal lattice during growth, yielding p-type and n-type semiconductors, respectively (ref. 46 and references therein). However, this can be achieved only during CVD bulk crystal growth, which is inherently a slow process. Controlled incorporation of dopants, not to mention spatially selective doping, for 2D MX₂ still remains to be established.

An alternative solution to controllable doping in 2D crystals is charge transfer doping through interaction with adlayers, atoms or molecules. Charge transfer can lead to either electron or hole doping depending on the reduction potential of the doping species with respect to the chemical potential of the semiconductor (Fig. 8). Charge transfer doping occurs *via* injection (extraction) of electrons into (from) the conduction or valence band of the material, leading to a change in free carrier density and a corresponding change in electrical conductivity. Versatile doping *via* charge transfer enables the optimization of MX₂ device performances as well as the development of sensors with ultra-high sensitivity.

9.1 Electron donors and acceptors

Charge transfer doping has been used to induce electron or hole doping in a variety of nanomaterials including graphene^{141–145} and carbon nanotubes.^{146–148} For MX₂, a variety of reducing agents, such as alkali metals,¹⁴⁹ ammonia,⁷⁷ amines,¹⁵⁰ and imines,¹⁵¹ the biological cofactor nicotinamide adenine dinucleotide (NADH),¹⁴⁰ tetrathiafulvalene (TTF),¹⁵² and benzyl viologen (BV),¹³⁹ have been used to modify the carrier density by n-type doping. Oxidizing agents such as NO,²⁰ NO₂,^{36,77} O₂,^{153,154} tetracyanoquinodimethanes (TCNQ and its tetrafluoro analogue F₄TCNQ),¹⁴⁰ gold salts (AuCl₃)^{19,155} and metal oxides (MoO₃)¹⁵⁶ were found to induce p-type doping. Other compounds such as tetracyanoethylene (TCNE),¹⁵² dichlorobenzene (DCB), dichloropentane (DCP), nitro-toluene (NT), nitromethane (NM)¹⁵⁰ and carbon fullerene (C₆₀)¹⁵⁶ were found to have no effect on the conductivity of MX₂, which may be explained by a weaker interaction with the surface^{152,156} and a high energy barrier opposing the electron transfer. Water has been

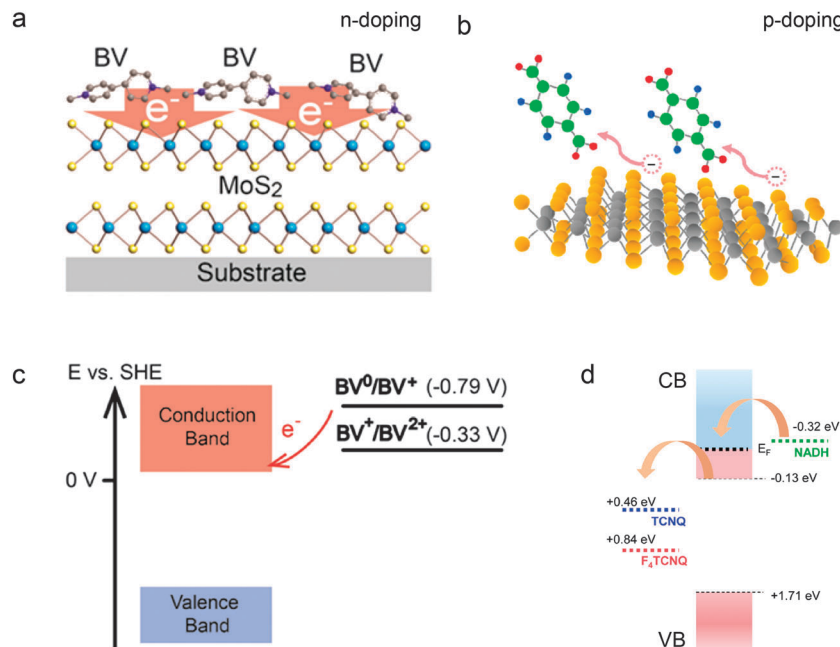


Fig. 8 Charge transfer doping. Schematic representation of the molecular charge transfer mechanism leading to (a) electron-doping or (b) hole-doping in MoS₂. (c and d) Redox potentials of the species used for charge transfer doping with respect to the conduction band edge (BV, benzylviologen; NADH, nicotinamide adenine dinucleotide; TCNQ, 7,7,8,8-tetracyanoquinodimethane; F₄TCNQ, 2,3,5,6-tetrafluoro-7,7,8,8-tetracyanoquinodimethane). (a and c) Reprinted with permission from ref. 139. Copyright 2014 American Chemical Society. (b and d) Reprinted with permission from ref. 140. Copyright 2013 American Chemical Society.

reported to behave as a p-type dopant for MoS₂¹⁵³ but there are also contradicting reports on its effects.¹⁵⁰ Types of dopants for MX₂ and their effects are summarized in Table 1.

Although the relative position of the reduction potentials with respect to the chemical potential of MX₂ can be used to predict the dominant doping type (Fig. 9), the extent to which the dopant molecules can interact with the MX₂ surface ultimately determines if doping will occur at all, whether it is reversible²⁰ and the maximum achievable doping density. Charge transfer doping in the above examples involves a reversible physisorption process that is not based on the covalent chemical modification of the MX₂ surfaces.^{77,139} Below we discuss examples and characteristics of volatile, non-volatile, and intercalation-based doping schemes.

9.2 Non-volatile doping

Stable charge transfer doping can be achieved by coating the MX₂ surface with adlayers of various organic and inorganic compounds. Recent demonstrations include SiN_x on WSe₂,¹⁵⁷ Cs₂CO₃,¹⁵⁸ and MoO_x¹⁵⁶ on MoS₂, and ZrO₂ as a top-gate insulator for both MoS₂ and WSe₂.^{36,139,159} n-Type doping of few-layer MoS₂ by physisorption has been achieved by immersing the sample in a solution of polyethyleneimine (PEI)¹⁵¹ or benzylviologen.¹³⁹ In the latter case, the doping was found to be reversible upon rinsing in toluene. Both n-type and p-type doping can be realized by simply drop-casting solutions of NADH and TCNQ, respectively, on monolayer MoS₂.¹⁴⁰ An alternative approach involving modification of the substrate prior to deposition of MX₂ layers has not been explored for

charge transfer doping, although various coatings on SiO_x are known to improve the device performance.^{39,122,123,125} The combination of adlayer deposition and substrate modification possibly allows fine control of doping densities over a wide range. Recent demonstration of defect ‘healing’ on both top and bottom sides of monolayer MoS₂ offers insights in this direction.⁹⁶

Degenerate doping of the contact regions of MX₂ FET devices has proved to be effective in minimizing the Schottky barrier and lowering the contact resistance. This was achieved by exposing the contact regions to NO₂ gas³⁶ (Fig. 10a), potassium vapour¹⁵⁹ (Fig. 10b), or to a solution of benzyl viologen.¹³⁹ Similarly, insertion of a thin MoO_x layer, a strongly electron withdrawing compound, at the interface between the metal electrode and MX₂ has also shown to enable effective hole injection into the channel.¹⁶⁰ This technique is compatible with the standard lithography processes thus allowing spatially selective doping of the MX₂ layer. A contact resistance as low as $\sim 0.5 \Omega \text{ mm}$ has been achieved for few-layer WSe₂ and MoS₂ by charge transfer doping (see ref. 161 and references therein).

These doping schemes are non-volatile in that they are stable in the absence of further processes (*e.g.* exposure to solvents, decomposition of the dopant species due to oxidation, and changes in temperature and atmospheric pressure). However, they are not stable enough to ensure reliability in long-term operation of FETs under ambient conditions. For device applications, novel strategies that allow stable doping against changes in environmental factors such as temperature and humidity are needed.

Table 1 Chemicals used for charge transfer doping of TMDs. NADH, nicotinamide adenine dinucleotide; NH₃, ammonia; TEA, triethylamine; THF, tetrahydrofuran; PEI, polyethyleneimine; TTF, tetrathiafulvalene; CsCO₃, cesium carbonate; K, potassium; BV, benzyl viologen; TCNE, tetracyanoethylene; H₂O, water; DCB, dichlorobenzene; DCP, dichloropentane; NT, nitrotoluene; NM, nitromethane; C₆₀, [60] fullerene; NO, nitrogen monoxide; F₄TCNQ, 2,3,5,6-tetrafluoro-7,7,8,8-tetracyanoquinodimethane; TCNQ, 7,7,8,8-tetracyanoquinodimethane; AuCl₃, gold chloride; O₂, oxygen; NO₂, nitrogen dioxide; MoO₃, molybdenum trioxide

Dopant	Coating	Doping	Mechanism	TMD	Ref.
NADH	-	n	Charge transfer (reduction)	MoS ₂	(140)
NH ₃					(77)
TEA, THF					(150)
PEI					(151)
TTF					(152)
CsCO ₃	CsCO ₃				(157)
K	(158)				
BV	ZrO ₂			WSe ₂	(158)
TCNE	MoS ₂			(139)	
H ₂ O, DCB, DCP, NT, NM	No effect		MoS ₂	(152)	
C ₆₀	C ₆₀	p	Unclear Charge transfer (oxidation)	MoS ₂	(150)
NO	(20)				
F ₄ TCNQ, TCNQ	(140)				
AuCl ₃	(155)				
H ₂ O, O ₂	MoSe ₂			(153)	
NO ₂	WSe ₂			(153)	
	ZrO ₂			MoS ₂	(77)
				WSe ₂	(36)
				MoS ₂	(156)
MoO ₃	MoO ₃			MoS ₂	(156)

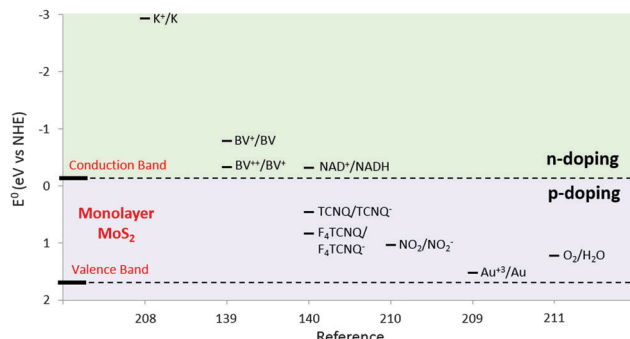


Fig. 9 Redox potential. Standard reduction potentials of chemicals used for charge-transfer doping of TMDs and the energy level of the valence and conduction band edges of monolayer MoS₂. BV, benzyl viologen; NADH, nicotinamide adenine dinucleotide; TCNQ, 7,7,8,8-tetracyanoquinodimethane; F₄TCNQ, 2,3,5,6-tetrafluoro-7,7,8,8-tetracyanoquinodimethane. The electrochemical potentials were obtained from ref. 139, 140, 208–211.

9.3 Volatile doping

It is well established that the electrical properties of MX₂ sensitively depend on the gaseous environment¹⁶² (Fig. 7c). While charge transfer from the gas molecules to MX₂ may occur *via* surface adsorption, electrostatic stabilization of polar molecules or ions can lead to temporary or “volatile” doping. In this case, MX₂ immediately becomes undoped once the supply of the gas is terminated. Since the PL intensity of monolayer MX₂ is strongly dependent on doping density, changes in the doping level can be monitored *in situ*. A report by Tongay *et al.*¹⁵³ indicates that water effectively induces strong p-type doping similar to oxygen but at 50 time lower concentrations (Fig. 11a).

Similarly, gaseous nitric oxide (NO₂) and ammonia (NH₃) were found to induce volatile n-type and p-type doping, respectively, in monolayer CVD MoS₂ (Fig. 11c and d).⁷⁷ High sensitivity to triethylamine (TEA) vapour and other volatile chemicals such as tetrahydrofuran (THF) and acetone (all polar molecules) has also been reported for mechanically exfoliated monolayer MoS₂¹⁵⁰ (Fig. 11e). Interestingly, however, no response to water vapour was observed in this study.

9.4 Reductive intercalation and phase transition

Reductive intercalation of bulk MX₂ materials with alkali metal ions leads to a drastic increase in conductivity of the host material.¹⁶³ In fact, several intercalation complexes of MoS₂ such as K_{0.4}MoS₂ and Na_{0.6}MoS₂ are known to be superconductors.^{149,164} Intercalation by alkali metal ions can be achieved by exposing MX₂ to alkyl lithium reagents^{163,165} or reducing salts (*i.e.* LiBH₄)¹⁶⁶. The negative charge transferred from the C-Li bond to the TMD basal planes is electrostatically balanced by the alkali metal cations, inducing disruption of the van der Waals interlayer adhesion forces. The carrier densities in these intercalation complexes typically range between $3 \sim 10 \times 10^{14} \text{ cm}^{-2}$, significantly larger than those commonly achieved by charge transfer doping of monolayer MX₂.

In the electrochemical analogue, the reduction is accompanied by the intercalation of positively charged counterions from the supporting electrolyte.¹⁶⁷ In this case, the electron donor is the electrode metal, which is driven by an applied bias, and the metal ions contribute by stabilizing the extra charge introduced to the MX₂ layers.

Alkali metal intercalation is often accompanied by a 2H-to-1T phase transition in MX₂.^{168–174} This phase transition, which was

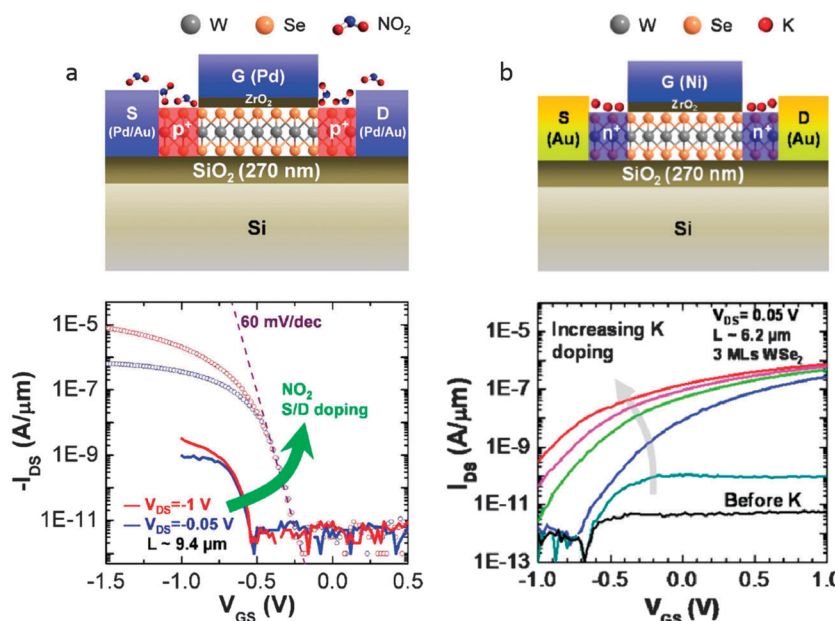


Fig. 10 Spatially selective doping. By selectively (a) p- and (b) n-doping a WSe₂ FET near the source and drain electrodes (left), the Schottky barrier to injection of holes and electrons, respectively, is minimized. The doping determines the polarity of the devices and a remarkable increase of the on-current (right). (a) Reprinted with permission from ref. 36. Copyright 2012 American Chemical Society. (b) Reprinted with permission from ref. 159. Copyright 2013 American Chemical Society.

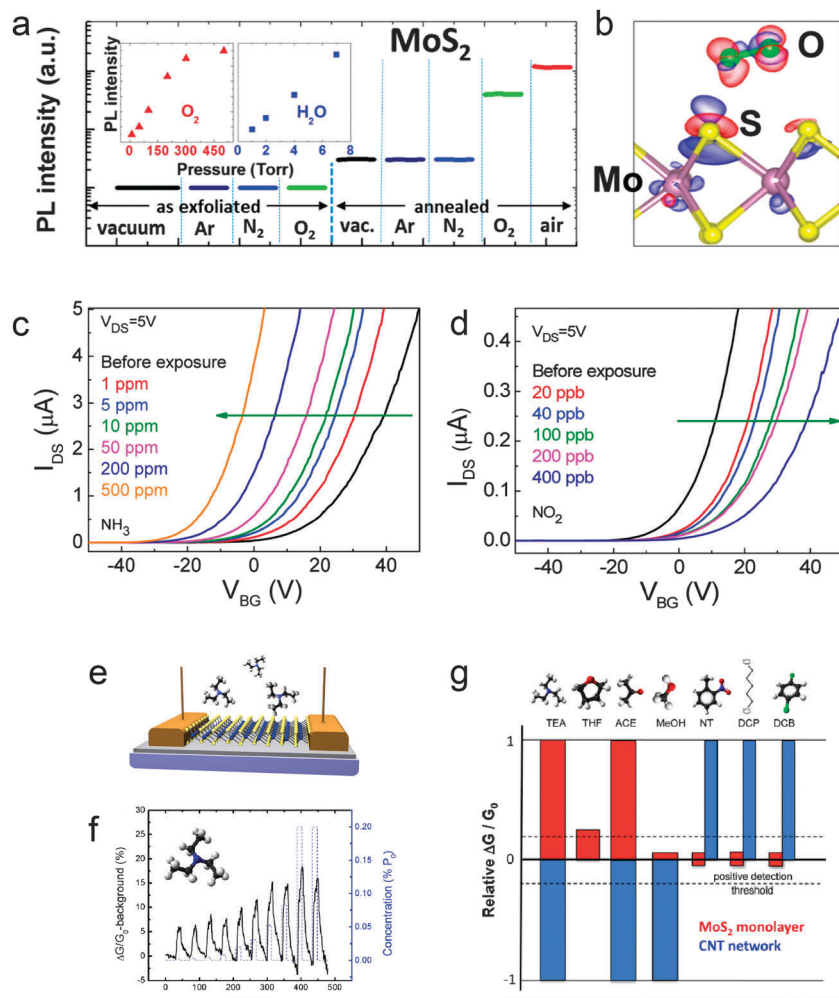


Fig. 11 Gas doping. (a) Modulation of PL intensity of monolayer MoS₂ during exposure to O₂, water or air. Note the 50-fold greater influence from water (insets) and the lack of response prior to thermal annealing. (b) Effect of O₂ adsorption on the TMD surface charge density predicted by density functional theory (DFT) calculations. (c and d) Effect of n-type and p-type doping induced by different concentrations of ammonia (NH₃) and nitric oxide (NO₂), respectively, on the threshold voltage of a monolayer MoS₂ FET. (e) Schematic of a TMD gas sensor. (f) Conductance changes as a function of exposure time to increasing concentrations of triethylamine (TEA). (g) Sensitivity of monolayer MoS₂ (red) to various analytes (TEA, triethylamine; THF, tetrahydrofuran; ACE: acetone; MeOH, methanol; DCP, dichloropentane; DCB, dichlorobenzene). Data for carbon nanotube network FETs are also shown for comparison (blue). (a and b) Reprinted with permission from ref. 153. Copyright 2013 American Chemical Society. (c and d) Reprinted with permission from ref. 77. Copyright 2013 American Chemical Society. (e–g) Reprinted with permission from ref. 150. Copyright 2014 American Chemical Society.

also observed to occur under electron irradiation,¹⁷⁵ leads to a drastic increase in electrical conductivity due to semiconductor-to-metal transition (see Fig. 1c and d for the electronic structure of the two phases). Kappera *et al.*¹⁷⁶ recently showed that the 1T-2H junction exhibits remarkably low contact resistance and thus is helpful for realizing high performance MX₂ FET devices.

10. Future outlook

Chemical approaches to doping and modifying TMDs offer viable routes to optimizing their properties for device applications. While recently explored strategies relying on the physisorption of oxidizing or reducing species on MX₂ surfaces have shown some promise, long-term stability remains a challenge.

Below we discuss prospects on controlled doping *via* chemical modification of the substrate and the MX₂ surface, with the aim to offer some insight into how lessons learned from other materials can be applied to the development of applications for MX₂ FETs.

10.1 Self-assembled monolayers

Self-assembled monolayers (SAMs) of alkoxysilanes on the SiO₂ surface¹⁷⁷ were previously shown to allow stable doping of graphene.^{134,178,179} The use of SAM dipoles remains largely unexplored for MX₂ devices.¹⁸⁰ SAM modification of the substrate is a technique for passivating the charged impurities on the substrate as well as tuning the carrier density in the channel. This versatile approach to substrate surface modification is also practical from a scalability point of view.

The formation of SAMs on the MX_2 FET channel surface is an alternative approach involving derivatization of TMD surfaces. This can be achieved by using alkylthiol compounds. Makarova *et al.*⁹⁷ showed that the sulfur in the thiol group binds to transition metal atoms which are not fully coordinated due to sulfur vacancies in MoS_2 . The authors showed that current pulses applied *via* an STM tip desulfurize the alkyl moieties while leaving the sulfur in place, thus resulting in effective ‘healing’ of sulfur vacancies through this procedure. By adapting this method to treat both sides of the MoS_2 monolayer, Yu *et al.*⁹⁶ achieved one of the highest room temperature mobilities so far reported. These authors also showed that the use of thiols with acidic (electron-withdrawing) groups (such as the silanol moiety resulting from the hydrolysis of mercaptopropyltrimethoxysilane) lowers the activation energy needed to break the S–C bond, allowing vacancy ‘healing’ to be performed on the whole sample using a simple thermal annealing treatment. Such a healing is particularly relevant in reducing short-range scatterers, which are believed to be one of the dominant scattering centers in high mobility devices. Moehl *et al.*¹⁸¹ found that the amino acid cysteine interacts with both the metal atom dangling bonds at the edge sites and with the lone pair of the d_{z^2} orbital, therefore greatly influencing the carrier lifetimes in the material. Recent findings also indicate that the self-assembly of amines on MX_2 surfaces represents an alternative route to thiol-based chemical derivatization of these materials.

10.2 Functional adlayers

It was recently shown that monolayer MoS_2 FET coated with a 7 nm-thick CsCO_3 adlayer is sensitive to air exposure.¹⁵⁸ This finding suggests that surface adsorbates can be indirectly sensed by the channel material, which is buried below the adlayer. This opens up new possibilities for tailoring the surface reactivity and functionalities of MX_2 . The use of ‘buffer’ adlayers may be a viable strategy for realizing stable sensors with high selectivity towards specific molecular targets. Thin oxide coatings (Al_2O_3 ,¹⁸² MoO_3 ,¹⁵⁶ ZrO_2 ,^{36,159} and $\text{SiO}_2/\text{ZrO}_2$ ¹³⁹) would enable the use of well-established protocols based on silane¹⁸³ or phosphonate^{184–186} SAMs to decorate the channel with chemical handles.

Similarly, the possibility of charge transfer by tunneling through thin dielectrics^{187–192} could allow the use of electrochemical techniques for derivatizing the surface of the adlayer,^{193,194} without direct modification of the TMD material. Representative electrochemical techniques that may be useful include electrogelation,^{195,196} electrografting¹⁹⁷ (for example aryl diazonium salts,¹⁹⁸), localized click-reactions,^{199,200} and electrodeposition.²⁰¹

10.3 Sensing applications

As demonstrated previously in silicon nanowire sensors,^{202–205} chemical modification of the semiconductor surface (chemisorption) is a promising route for achieving stable FET operations and targeted sensing. The ability to precisely tailor the chemistry of the surface functional groups will open up opportunities for sensing in complex mixtures of analytes such as biological fluids.

The 2D nature of TMDs is suitable for realizing multiplexed sensor arrays where each sensing element bears recognition moieties for specific analytes.^{206,207}

11. Conclusion

Recent advances in 2D TMD field effect devices point to promising prospects for the development of novel applications. Electronic transport measurements provide a powerful tool for probing various surface and interface effects. Studies to date indicate that there is still significant room for improving the device performance and exploring new functionalities. In this regard, chemistry of surfaces and interfaces plays a crucial role in optimizing injection and transport of charges across the device. Surface charge transfer doping and functionalization of 2D TMDs offer a remarkably versatile approach to tailoring these materials for application in solid state electronics and sensing.

Notes added in proof

During the submission of this Review Article, high mobility MoS_2 FETs were reported by Cui *et al.*²¹² The authors demonstrated low temperature mobility of up to $10\,000\,\text{cm}^2\,\text{V}^{-1}\,\text{s}^{-1}$ for few layer MoS_2 encapsulated between hBN layers and contacted by graphene. These values are not included in Fig. 6.

Acknowledgements

This research is supported by the National Research Foundation (NRF), Prime Minister’s Office, Singapore under its Medium sized centre programme as well as NRF Research fellowship (NRF-NRFF2011-02).

References

- 1 K. S. Novoselov, A. K. Geim, S. V. Morozov, D. Jiang, Y. Zhang, S. V. Dubonos, I. V. Grigorieva and A. A. Firsov, Electric Field Effect in Atomically Thin Carbon Films, *Science*, 2004, **306**, 666.
- 2 K. S. Novoselov, D. Jiang, F. Schedin, T. J. Booth, V. V. Khotkevich, S. V. Morozov and A. K. Geim, Two-dimensional atomic crystals, *Proc. Natl. Acad. Sci. U. S. A.*, 2005, **102**, 10451.
- 3 Graphene is not alone, Editorial, *Nature Nanotechnology*, 2012, **7**, 683.
- 4 Z. Zeng, Z. Yin, X. Huang, H. Li, Q. He, G. Lu, F. Boey and H. Zhang, Single-Layer Semiconducting Nanosheets: High-Yield Preparation and Device Fabrication, *Angew. Chem., Int. Ed.*, 2011, **50**, 11093.
- 5 H. O. H. Churchill and P. Jarillo-Herrero, Two-dimensional crystals: Phosphorus joins the family, *Nat. Nanotechnol.*, 2014, **9**, 330.
- 6 Q. H. Wang, K. Kalantar-Zadeh, A. Kis, J. N. Coleman and M. S. Strano, Electronics and optoelectronics of two-dimensional

- transition metal dichalcogenides, *Nat. Nanotechnol.*, 2012, **7**, 699.
- 7 A. K. Geim and I. V. Grigorieva, Van der Waals heterostructures, *Nature*, 2013, **499**, 419.
 - 8 V. Nicolosi, M. Chhowalla, M. G. Kanatzidis, M. S. Strano and J. N. Coleman, Liquid Exfoliation of Layered Materials, *Science*, 2013, **340**, 6139.
 - 9 S. Z. Butler, S. M. Hollen, L. Cao, Y. Cui, J. A. Gupta, H. R. Gutierrez, T. F. Heinz, S. S. Hong, J. Huang, A. F. Ismach, E. Johnston-Halperin, M. Kuno, V. V. Plashnitsa, R. D. Robinson, R. S. Ruoff, S. Salahuddin, J. Shan, L. Shi and M. G. Spencer, *et al.*, Progress, Challenges, and Opportunities in Two-Dimensional Materials Beyond Graphene, *ACS Nano*, 2013, **7**, 2898.
 - 10 D. Jariwala, V. K. Sangwan, L. J. Lauhon, T. J. Marks and M. C. Hersam, Emerging Device Applications for Semiconducting Two-Dimensional Transition Metal Dichalcogenides, *ACS Nano*, 2014, **8**, 1102.
 - 11 L. Britnell, R. M. Ribeiro, A. Eckmann, R. Jalil, B. D. Belle, A. Mishchenko, Y.-J. Kim, R. V. Gorbachev, T. Georgiou, S. V. Morozov, A. N. Grigorenko, A. K. Geim, C. Casiraghi, A. H. Castro Neto and K. S. Novoselov, Strong Light-Matter Interactions in Heterostructures of Atomically Thin Films, *Science*, 2013, **340**, 1311.
 - 12 B. Radisavljevic, A. Radenovic, J. Brivio, V. Giacometti and A. Kis, Single-layer MoS₂ transistors, *Nat. Nanotechnol.*, 2011, **6**, 147.
 - 13 K. F. Mak, C. Lee, J. Hone, J. Shan and T. F. Heinz, Atomically Thin MoS₂: A New Direct-Gap Semiconductor, *Phys. Rev. Lett.*, 2010, **105**, 136805.
 - 14 J. T. Ye, Y. J. Zhang, R. Akashi, M. S. Bahramy, R. Arita and Y. Iwasa, Superconducting Dome in a Gate-Tuned Band Insulator, *Science*, 2012, **338**, 1193.
 - 15 Z. Yin, H. Li, H. Li, L. Jiang, Y. Shi, Y. Sun, G. Lu, Q. Zhang, X. Chen and H. Zhang, Single-Layer MoS₂ Phototransistors, *ACS Nano*, 2012, **6**, 74.
 - 16 D. Xiao, G.-B. Liu, W. Feng, X. Xu and W. Yao, Coupled Spin and Valley Physics in Monolayers of MoS₂ and Other Group-VI Dichalcogenides, *Phys. Rev. Lett.*, 2012, **108**, 196802.
 - 17 K. Gong, L. Zhang, D. Liu, L. Liu, Y. Zhu, Y. Zhao and H. Guo, Electric control of spin in monolayer WSe₂ field-effect transistors, *Nanotechnology*, 2014, **25**, 435201.
 - 18 Y. Yoon, K. Ganapathi and S. Salahuddin, How Good Can Monolayer MoS₂ Transistors Be?, *Nano Lett.*, 2011, **11**, 3768.
 - 19 M. S. Choi, D. Qu, D. Lee, X. Liu, K. Watanabe, T. Taniguchi and W. J. Yoo, Lateral MoS₂ p-n Junction Formed by Chemical Doping for Use in High-Performance Optoelectronics, *ACS Nano*, 2014, **8**, 9332.
 - 20 H. Li, Z. Yin, Q. He, H. Li, X. Huang, G. Lu, D. W. H. Fam, A. L. Y. Tok, Q. Zhang and H. Zhang, Fabrication of Single- and Multilayer MoS₂ Film-Based Field-Effect Transistors for Sensing NO at Room Temperature, *Small*, 2012, **8**, 63.
 - 21 Q. He, Z. Zeng, Z. Yin, H. Li, S. Wu, X. Huang and H. Zhang, Fabrication of Flexible MoS₂ Thin-Film Transistor Arrays for Practical Gas-Sensing Applications, *Small*, 2012, **8**, 2994.
 - 22 C. Zhu, Z. Zeng, H. Li, F. Li, C. Fan and H. Zhang, Single-Layer MoS₂-Based Nanoprobes for Homogeneous Detection of Biomolecules, *J. Am. Chem. Soc.*, 2013, **135**, 5998.
 - 23 J. Pu, Y. Yomogida, K.-K. Liu, L.-J. Li, Y. Iwasa and T. Takenobu, Highly Flexible MoS₂ Thin-Film Transistors with Ion Gel Dielectrics, *Nano Lett.*, 2012, **12**, 4013.
 - 24 J. Pu, L.-J. Li and T. Takenobu, Flexible and stretchable thin-film transistors based on molybdenum disulphide, *Phys. Chem. Chem. Phys.*, 2014, **16**, 14996.
 - 25 R. Fivaz and E. Mooser, Mobility of Charge and Carriers in Semiconducting and Layer Structures, *Phys. Rev.*, 1967, **163**, 3.
 - 26 R. F. Frindt, Single Crystals of MoS₂ Several Molecular Layers Thick, *J. Appl. Phys.*, 1966, **37**, 1928.
 - 27 P. Joensen, R. F. Frindt and S. R. Morrison, Single layer MoS₂, *Mater. Res. Bull.*, 1986, **21**, 457.
 - 28 W. M. R. Divigalpitiya, S. R. Morrison and R. F. Frindt, Thin oriented films of molybdenum disulphide, *Thin Solid Films*, 1990, **186**, 177.
 - 29 V. Podzorov, M. E. Gershenson, C. H. Kloc, R. Zeis and E. Bucher, High-mobility field-effect transistors based on transition metal dichalcogenides, *Appl. Phys. Lett.*, 2004, **84**, 3301.
 - 30 A. Ayari, E. Cobas, O. Ogundadegbe and M. S. Fuhrer, Realization and electrical characterization of ultrathin crystals of layered transition-metal dichalcogenides, *J. Appl. Phys.*, 2007, **101**, 014507.
 - 31 B. Radisavljevic, M. B. Whitwick and A. Kis, Integrated Circuits and Logic Operations Based on Single-Layer MoS₂, *ACS Nano*, 2011, **5**, 9934.
 - 32 X. Wang, Y. Gong, G. Shi, W. L. Chow, K. Keyshar, G. Ye, R. Vajtai, J. Lou, Z. Liu, E. Ringe, B. K. Tay and P. M. Ajayan, Chemical Vapor Deposition Growth of Crystalline Monolayer MoSe₂, *ACS Nano*, 2014, **8**, 5125.
 - 33 S. Larentis, B. Fallahazad and E. Tutuc, Field-effect transistors and intrinsic mobility in ultra-thin MoSe₂ layers, *Appl. Phys. Lett.*, 2012, **101**, 223104.
 - 34 N. R. Pradhan, D. Rhodes, Y. Xin, S. Memaran, L. Bhaskaran, M. Siddiq, S. Hill, P. M. Ajayan and L. Balicas, Ambipolar Molybdenum Diselenide Field-Effect Transistors: Field-Effect and Hall Mobilities, *ACS Nano*, 2014, **8**, 7923.
 - 35 A. Allain and A. Kis, Electron and Hole Mobilities in Single-Layer WSe₂, *ACS Nano*, 2014, **8**, 7180.
 - 36 H. Fang, S. Chuang, T. C. Chang, K. Takei, T. Takahashi and A. Javey, High-Performance Single Layered WSe₂ p-FETs with Chemically Doped Contacts, *Nano Lett.*, 2012, **12**, 3788.
 - 37 D. Ovchinnikov, A. Allain, Y.-S. Huang, D. Dumcenco and A. Kis, Electrical Transport Properties of Single-Layer WS₂, *ACS Nano*, 2014, **8**, 8174.
 - 38 S. Jo, N. Ubrig, H. Berger, A. B. Kuzmenko and A. F. Morpurgo, Mono- and Bilayer WS₂ Light-Emitting Transistors, *Nano Lett.*, 2014, **14**, 2019.
 - 39 F. Withers, T. H. Bointon, D. C. Hudson and M. F. Craciun, Saverio Russo, Electron transport of WS₂ transistors in a hexagonal boron nitride dielectric environment, *Sci. Rep.*, 2014, **4**, 4967.

- 40 Y.-F. Lin, Y. Xu, S.-T. Wang, S.-L. Li, M. Yamamoto, A. Aparecido-Ferreira, W. Li, H. Sun, S. Nakaharai, W.-B. Jian, K. Ueno and K. Tsukagoshi, Ambipolar MoTe₂ Transistors and Their Applications in Logic Circuits, *Adv. Mater.*, 2014, **26**, 3263.
- 41 I. Gutierrez Lezama, A. Arora, A. Ubaldini, C. Barreteau, E. Giannini, M. Potemski and A. F. Morpurgo, Indirect-to-Direct Band Gap Crossover in Few-Layer MoTe₂, *Nano Lett.*, 2015, **15**, 2336.
- 42 J. H. Han, S. Lee, D. Yoo, J.-H. Lee, S. Jeong, J.-G. Kim and J. Cheon, Unveiling Chemical Reactivity and Structural Transformation of Two-Dimensional Layered Nanocrystals, *J. Am. Chem. Soc.*, 2013, **135**, 3736.
- 43 H. Liu, A. T. Neal, Z. Zhu, Z. Luo, X. Xu, D. Tománek and P. D. Ye, Phosphorene: An Unexplored 2D Semiconductor with a High Hole Mobility, *ACS Nano*, 2014, **8**, 4033.
- 44 L. Li, Y. Yu, G. J. Ye, Q. Ge, X. Ou, H. Wu, D. Feng, X. H. Chen and Y. Zhang, Black phosphorus field-effect transistors, *Nat. Nanotechnol.*, 2014, **9**, 372.
- 45 S. P. Koenig, R. A. Doganov, H. Schmidt, A. H. Castro Neto and B. Ozyilmaz, Electric field effect in ultrathin black phosphorus, *Appl. Phys. Lett.*, 2014, **104**, 103106.
- 46 J. A. Yoffe and A. D. Wilson, The transition metal dichalcogenides discussion and interpretation of the observed optical, electrical and structural properties, *Adv. Phys.*, 1969, **18**, 193.
- 47 R. B. Murray, R. A. Bromley and A. D. Yoffe, The band structures of some transition metal dichalcogenides. II. Group IVA; octahedral coordination, *J. Phys. C: Solid State Phys.*, 1972, **5**, 746.
- 48 R. A. Bromley, R. B. Murray and A. D. Yoffe, The band structures of some transition metal dichalcogenides. III. Group VIA: trigonal prism materials, *J. Phys. C: Solid State Phys.*, 1972, **5**, 759.
- 49 R. M. A. Lieth and J. C. J. M. Terhell, Preparation and crystal growth of materials with layered structures, in *Physics and Chemistry of Materials with Layered Structures*, ed. R. M. A. Lieth, 1977.
- 50 B. W. H. Baugher, H. O. H. Churchill, Y. Yang and P. Jarillo-Herrero, Intrinsic Electronic Transport Properties of High-Quality Monolayer and Bilayer MoS₂, *Nano Lett.*, 2013, **13**, 4212.
- 51 M. Chhowalla, H. S. Shin, G. Eda, L.-J. Li, K. P. Loh and H. Zhang, The chemistry of two-dimensional layered transition metal dichalcogenide nanosheets, *Nat. Chem.*, 2013, **5**, 263.
- 52 W. Zhao, R. Mendes Ribeiro and G. Eda, Electronic Structure and Optical Signatures of Semiconducting Transition Metal Dichalcogenide Nanosheets, *Acc. Chem. Res.*, 2015, **48**, 91.
- 53 S.-L. Li, H. Miyazaki, H. Song, H. Kuramochi, S. Nakaharai and K. Tsukagoshi, Quantitative Raman Spectrum and Reliable Thickness Identification for Atomic Layers on Insulating Substrates, *ACS Nano*, 2012, **6**, 7381.
- 54 W. Zhao, Z. Ghorannevis, K. K. Amara, J. R. Pang, M. Toh, X. Zhang, C. Kloc, P. H. Tan and G. Eda, Lattice dynamics in mono- and few-layer sheets of WS₂ and WSe₂, *Nanoscale*, 2013, **5**, 9677.
- 55 H. J. Conley, B. Wang, J. I. Ziegler, R. F. Haglund, S. T. Pantelides and K. I. Bolotin, Bandgap Engineering of Strained Monolayer and Bilayer MoS₂, *Nano Lett.*, 2013, **13**, 3626.
- 56 A. Castellanos-Gomez, R. Roldán, E. Cappelluti, M. Buscema, F. Guinea, H. S. J. van der Zant and G. A. Steele, Local Strain Engineering in Atomically Thin MoS₂, *Nano Lett.*, 2013, **13**, 5361.
- 57 D. Sercombe, S. Schwarz, O. Del Pozo-Zamudio, F. Liu, B. J. Robinson, E. A. Chekhovich, I. I. Tartakovskii, O. Kolosov and A. I. Tartakovskii, Optical investigation of the natural electron doping in thin MoS deposited on dielectric substrates, *Sci. Rep.*, 2013, **3**, 3489.
- 58 J. Zheng, H. Zhang, S. Dong, Y. Liu, C. T. Nai, H. S. Shin, H. Y. Jeong, B. Liu and K. P. Loh, High yield exfoliation of two-dimensional chalcogenides using sodium naphthalenide, *Nat. Commun.*, 2014, **5**, 2995.
- 59 K. K. Amara, L. Chu, R. Kumar, M. Toh and G. Eda, Wet chemical thinning of molybdenum disulfide down to its monolayer, *APL Mater.*, 2014, **2**, 092509.
- 60 Y. Huang, J. Wu, X. Xu, Y. Ho, G. Ni, Q. Zou, G. K. W. Koon, W. Zhao, A. H. Castro Neto, G. Eda, C. Shen and B. Özyilmaz, An innovative way of etching MoS₂: Characterization and mechanistic investigation, *Nano Res.*, 2013, **6**, 200.
- 61 Y. Liu, H. Nan, X. Wu, W. Pan, W. Wang, J. Bai, W. Zhao, L. Sun, X. Wang and Z. Ni, Layer-by-Layer Thinning of MoS₂ by Plasma, *ACS Nano*, 2013, **7**, 4202.
- 62 A. Castellanos-Gomez, M. Barkelid, A. M. Goossens, V. E. Calado, H. S. J. van der Zant and G. A. Steele, Laser-Thinning of MoS₂: On Demand Generation of a Single-Layer Semiconductor, *Nano Lett.*, 2012, **12**, 3187.
- 63 C. Altavilla, M. Sarno and P. Ciambelli, A Novel Wet Chemistry Approach for the Synthesis of Hybrid 2D Free-Floating Single or Multilayer Nanosheets of MS₂@oleylamine (M = Mo, W), *Chem. Mater.*, 2011, **23**, 3879.
- 64 L. K. Tan, B. Liu, J. H. Teng, S. Guo, H. Y. Low and K. P. Loh, Atomic layer deposition of a MoS₂ film, *Nanoscale*, 2014, **6**, 10584.
- 65 H. Schafer, *Chemical Transport Reactions*, Academic Press, New York, 1964.
- 66 Y. Zhan, Z. Liu, S. Najmaei, P. M. Ajayan and J. Lou, Large-Area Vapor-Phase Growth and Characterization of MoS₂ Atomic Layers on a SiO₂ Substrate, *Small*, 2012, **8**, 966.
- 67 K.-K. Liu, W. Zhang, Y.-H. Lee, Y.-C. Lin, M.-T. Chang, C.-Y. Su, C.-S. Chang, H. Li, Y. Shi, H. Zhang, C.-S. Lai and L.-J. Li, Growth of Large-Area and Highly Crystalline MoS₂ Thin Layers on Insulating Substrates, *Nano Lett.*, 2012, **12**, 1538.
- 68 Y.-H. Lee, X.-Q. Zhang, W. Zhang, M.-T. Chang, C.-T. Lin, K.-D. Chang, Y.-C. Yu, J. T.-W. Wang, C.-S. Chang, L.-J. Li and T.-W. Lin, Synthesis of Large-Area MoS₂ Atomic Layers with Chemical Vapor Deposition, *Adv. Mater.*, 2012, **24**, 2320.

- 69 M. Amani, M. L. Chin, A. G. Birdwell, T. P. O'Regan, S. Najmaei, Z. Liu, P. M. Ajayan, J. Lou and M. Dubey, Electrical performance of monolayer MoS₂ field-effect transistors prepared by chemical vapor deposition, *Appl. Phys. Lett.*, 2013, **102**, 193107.
- 70 A. M. van der Zande, P. Y. Huang, D. A. Chenet, T. C. Berkelsbach, Y. You, G.-H. Lee, T. F. Heinz, D. R. Reichman, D. A. Muller and J. C. Hone, Grains and grain boundaries in highly crystalline monolayer molybdenum disulphide, *Nat. Mater.*, 2013, **12**, 554.
- 71 H. Wang, L. Yu, Y.-H. Lee, Y. Shi, A. Hsu, M. L. Chin, L.-J. Li, M. Dubey, J. Kong and T. Palacios, Integrated Circuits Based on Bilayer MoS₂ Transistors, *Nano Lett.*, 2012, **12**, 4674.
- 72 S. Najmaei, Z. Liu, W. Zhou, X. Zou, G. Shi, S. Lei, B. I. Yakobson, J.-C. Idrobo, P. M. Ajayan and J. Lou, Vapour phase growth and grain boundary structure of molybdenum disulphide atomic layers, *Nat. Mater.*, 2013, **12**, 754.
- 73 Y. Yu, C. Li, Y. Liu, L. Su, Y. Zhang and L. Cao, Controlled Scalable Synthesis of Uniform, High-Quality Monolayer and Few-layer MoS₂ Films, *Sci. Rep.*, 2013, **3**, 1866.
- 74 C. Gong, C. Huang, J. Miller, L. Cheng, Y. Hao, D. Cobden, J. Kim, R. S. Ruoff, R. M. Wallace, K. Cho, X. Xu and Y. J. Chabal, Metal Contacts on Physical Vapor Deposited Monolayer MoS₂, *ACS Nano*, 2013, **7**, 11350.
- 75 Y. Liu, R. Ghosh, D. Wu, A. Ismach, R. Ruoff and K. Lai, Mesoscale Imperfections in MoS₂ Atomic Layers Grown by a Vapor Transport Technique, *Nano Lett.*, 2014, **14**, 4682.
- 76 H. Liu, M. Si, S. Najmaei, A. T. Neal, Y. Du, P. M. Ajayan, J. Lou and P. D. Ye, Statistical Study of Deep Submicron Dual-Gated Field-Effect Transistors on Monolayer Chemical Vapor Deposition Molybdenum Disulfide Films, *Nano Lett.*, 2013, **13**, 2640.
- 77 B. Liu, L. Chen, G. Liu, A. N. Abbas, M. Fathi and C. Zhou, High-Performance Chemical Sensing Using Schottky-Contacted Chemical Vapor Deposition Grown Monolayer MoS₂ Transistors, *ACS Nano*, 2014, **8**, 5304.
- 78 S. Najmaei, M. Amani, M. L. Chin, Z. g. Liu, A. G. Birdwell, T. P. O'Regan, P. M. Ajayan, M. Dubey and J. Lou, Electrical Transport Properties of Polycrystalline Monolayer Molybdenum Disulfide, *ACS Nano*, 2014, **8**, 7930.
- 79 H. Schmidt, S. Wang, L. Chu, M. Toh, R. Kumar, W. Zhao, A. H. Castro Neto, J. Martin, S. Adam, B. Özyilmaz and G. Eda, Transport Properties of Monolayer MoS₂ Grown by Chemical Vapor Deposition, *Nano Lett.*, 2014, **14**, 1909.
- 80 D. Dumcenco, D. Ovchinnikov, K. Marinov, O. Lopez-Sanchez, D. Krasnozhon, M.-W. Chen, P. Gillet, A. F. i Morral, A. Radenovic and A. Kis, Large-area Epitaxial Monolayer MoS, *ACS Nano*, 2015, **9**, 4611.
- 81 W. Zhu, T. Low, Y.-H. Lee, H. Wang, D. B. Farmer, J. Kong, F. Xia and P. Avouris, Electronic transport and device prospects of monolayer molybdenum disulphide grown by chemical vapour deposition, *Nat. Commun.*, 2014, **5**, 3087.
- 82 J. C. Shaw, H. Zhou, Y. Chen, N. O. Weiss, Y. Liu, Y. Huang and X. Duan, Chemical vapor deposition growth of monolayer MoSe and nanosheets, *Nano Res.*, 2014, **7**, 1.
- 83 Y. Zhang, Y. Zhang, Q. Ji, J. Ju, H. Yuan, J. Shi, T. Gao, D. Ma, M. Liu, Y. Chen, X. Song, H. Y. Hwang, Y. Cui and Z. Liu, Controlled Growth of High-Quality Monolayer WS₂ Layers on Sapphire and Imaging Its Grain Boundary, *ACS Nano*, 2013, **7**, 8963.
- 84 T. Tsirlina, V. Lyakhovitskaya, S. Fiechter and R. Tenne, Study on preparation, growth mechanism, and optoelectronic properties of highly oriented WSe₂ thin films, *J. Mater. Res.*, 2000, **15**, 2636.
- 85 J.-K. Huang, J. Pu, C.-L. Hsu, M.-H. Chiu, Z.-Y. Juang, Y.-H. Chang, W.-H. Chang, Y. Iwasa, T. Takenobu and L.-J. Li, Large-Area Synthesis of Highly Crystalline WSe₂ Monolayers and Device Applications, *ACS Nano*, 2014, **8**, 923.
- 86 Y. Gong, Z. Liu, A. R. Lupini, G. Shi, J. Lin, S. Najmaei, Z. Lin, A. L. Elías, A. Berkdemir, G. You, H. Terrones, M. Terrones, R. Vajtai, S. T. Pantelides, S. J. Pennycook, J. Lou, W. Zhou and P. M. Ajayan, Band Gap Engineering and Layer-by-Layer Mapping of Selenium-Doped Molybdenum Disulfide, *Nano Lett.*, 2014, **14**, 442.
- 87 Y.-C. Lin, D. O. Dumcenco, H.-P. Komsa, Y. Niimi, A. V. Krasheninnikov, Y.-S. Huang and K. Suenaga, Properties of Individual Dopant Atoms in Single-Layer MoS₂: Atomic Structure, Migration, and Enhanced Reactivity, *Adv. Mater.*, 2014, **18**, 2857.
- 88 H. Wang, L. Yu, Y.-H. Lee, W. Fang, A. Hsu, P. Herring, M. Chin, M. Dubey, L.-J. Li, J. Kong, T. Palacios, Large-scale 2D Electronics based on Single-layer MoS₂ Grown by Chemical Vapor Deposition, *Electron Devices Meeting (IEDM)*, 2012 IEEE International, 2012, p. 4.6.1.
- 89 J. Hong, Z. Hu, M. Probert, K. Li, D. Lv, X. Yang, L. Gu, N. Mao, Q. Feng, L. Xie, J. Zhang, D. Wu, Z. Zhang, C. Jin, W. Ji, X. Zhang, J. Yuan and Z. Zhang, Exploring atomic defects in molybdenum disulphide monolayers, *Nat. Commun.*, 2015, **6**, 6293.
- 90 W. Zhou, X. Zou, S. Najmaei, Z. Liu, Y. Shi, J. Kong, J. Lou, P. M. Ajayan, B. I. Yakobson and J.-C. Idrobo, Intrinsic Structural Defects in Monolayer Molybdenum Disulfide, *Nano Lett.*, 2013, **13**, 2615.
- 91 S. McDonnell, R. Addou, C. Buie, R. M. Wallace and C. L. Hinkle, Defect-Dominated Doping and Contact Resistance in MoS₂, *ACS Nano*, 2014, **8**, 2880.
- 92 C.-P. Lu, G. Li, J. Mao, L.-M. Wang and E. Y. Andrei, Bandgap, Mid-Gap States, and Gating Effects in MoS₂, *Nano Lett.*, 2014, **14**, 4628.
- 93 S. Tongay, J. Suh, C. Ataca, W. Fan, A. Luce, J. S. Kang, J. Liu, C. Ko, R. Raghunathanan, J. Zhou, F. Ogletree, J. Li, J. C. Grossman and J. Wu, Defects activated photoluminescence in two-dimensional semiconductors: interplay between bound, charged, and free excitons, *Sci. Rep.*, 2013, **3**, 2657.
- 94 S. Kim, A. Konar, W.-S. Hwang, J. H. Lee, J. Lee, J. Yang, C. Jung, H. Kim, J.-B. Yoo, J.-Y. Choi, Y. W. Jin, S. Y. Lee, D. Jena, W. Choi and K. Kim, High-mobility and low-power thin-film transistors based on multilayer MoS₂ crystals, *Nat. Commun.*, 2012, **3**, 1011.
- 95 H. Qiu, T. Xu, Z. Wang, W. Ren, H. Nan, Z. Ni, Q. Chen, S. Yuan, F. Miao, F. Song, G. Long, Y. Shi, L. Sun, J. Wang

- and X. Wang, Hopping transport through defect-induced localized states in molybdenum disulphide, *Nat. Commun.*, 2013, **4**, 2642.
- 96 Z. Yu, Y. Pan, Y. Shen, Z. Wang, Z.-Y. Ong, T. Xu, R. Xin, L. Pan, B. Wang, L. Sun, J. Wang, G. Zhang, Y. W. Zhang, Y. Shi and X. Wang, Towards intrinsic charge transport in monolayer molybdenum disulfide by defect and interface engineering, *Nat. Commun.*, 2014, **5**, 5290.
- 97 M. Makarova, Y. Okawa and M. Aono, Selective Adsorption of Thiol Molecules at Sulfur Vacancies on MoS₂(0001), Followed by Vacancy Repair via S-C Dissociation, *J. Phys. Chem. C*, 2012, **116**, 22411.
- 98 K. Liu, L. Zhang, T. Cao, C. Jin, D. Qiu, Q. Zhou, A. Zettl, P. Yang, S. G. Louie and F. Wang, Evolution of Interlayer Coupling in Twisted MoS₂ Bilayers, *Nat. Commun.*, 2014, **5**, 4966.
- 99 A. Castellanos-Gomez, H. S. J. van der Zant and G. A. Steele, Folded MoS and layers with reduced interlayer coupling, *Nano Res.*, 2014, **7**, 1.
- 100 H. Li, J. Wu, Z. Yin and H. Zhang, Preparation and Applications of Mechanically Exfoliated Single-Layer and Multilayer MoS₂ and WSe₂ Nanosheets, *Acc. Chem. Res.*, 2014, **47**, 1067.
- 101 S. Ghatak, A. N. Pal and A. Ghosh, Nature of Electronic States in Atomically Thin MoS₂ Field-Effect Transistors, *ACS Nano*, 2011, **5**, 7707.
- 102 A. T. Neal, H. Liu, J. Gu and P. D. Ye, Magneto-transport in MoS₂: Phase Coherence, Spin-Orbit Scattering, and the Hall Factor, *ACS Nano*, 2013, **7**, 7077.
- 103 M. S. Fuhrer and J. Hone, Measurement of mobility in dual-gated MoS₂ transistors, *Nat. Nanotechnol.*, 2013, **8**, 146.
- 104 M.-W. Lin, L. Liu, Q. Lan, X. Tan, K. S. Dhindsa, P. Zeng, V. M. Naik, M. M.-C. Cheng and Z. Zhou, Mobility enhancement and highly efficient gating of monolayer MoS and transistors with polymer, *J. Phys. D: Appl. Phys.*, 2012, **45**, 345102.
- 105 M. M. Perera, M.-W. Lin, H.-J. Chuang, B. P. Chamlagain, C. Wang, X. Tan, M. M.-C. Cheng, D. Tomanek and Z. Zhou, Improved Carrier Mobility in Few-Layer MoS₂ Field-Effect Transistors with Ionic-Liquid Gating, *ACS Nano*, 2013, **7**, 4449.
- 106 Y. J. Zhang, J. T. Ye, Y. Yomogida, T. Takenobu and Y. Iwasa, Formation of a Stable p-n Junction in a Liquid-Gated MoS₂ Ambipolar Transistor, *Nano Lett.*, 2013, **13**, 3023.
- 107 D. Braga, I. G. Lezama, H. Berger and A. F. Morpurgo, Quantitative Determination of the Band Gap of WS₂ with Ambipolar Ionic Liquid-Gated Transistors, *Nano Lett.*, 2012, **12**, 5218.
- 108 Y. Zhang, J. Ye, Y. Matsuhashi and Y. Iwasa, Ambipolar MoS₂ Thin Flake Transistors, *Nano Lett.*, 2012, **12**, 1136.
- 109 L. Chu, H. Schmidt, J. Pu, S. Wang, B. Özyilmaz, T. Takenobu and G. Eda, Charge transport in ion-gated mono-, bi-, and trilayer MoS₂ field effect transistors, *Sci. Rep.*, 2014, **4**, 7293.
- 110 D. K. Efetov and P. Kim, Controlling electron-phonon interactions in graphene at ultrahigh carrier densities, *Phys. Rev. Lett.*, 2010, **105**, 256805.
- 111 D. K. Efetov, P. Maher, S. Glinsky and P. Kim, Multiband transport in bilayer graphene at high carrier densities, *Phys. Rev. B: Condens. Matter Mater. Phys.*, 2011, **84**, 161412(R).
- 112 J. Ye, M. F. Craciunc, M. Koshino, S. Russo, S. Inoue, H. Yuan, H. Shimotani, A. F. Morpurgo and Y. Iwasa, Accessing the transport properties of graphene and its multilayers at high carrier density, *Proc. Natl. Acad. Sci. U. S. A.*, 2010, **108**, 13002.
- 113 B. Radisavljevic and A. Kis, Mobility engineering and a metal-insulator transition in monolayer MoS₂, *Nat. Mater.*, 2013, **12**, 815.
- 114 H.-J. Chuang, X. Tan, N. J. Ghimire, M. M. Perera, B. Chamlagain, M. M.-C. Cheng, J. Yan, D. Mandrus, D. Tomanek and Z. Zhou, High Mobility WSe₂ p- and n-Type Field-Effect Transistors Contacted by Highly Doped Graphene for Low-Resistance Contacts, *Nano Lett.*, 2014, **14**, 3594.
- 115 A. Castellanos-Gomez, E. Cappelluti, R. Roldán, N. Agrait, F. Guinea and G. Rubio-Bollinger, Electric-Field Screening in Atomically Thin Layers of MoS: the Role of Interlayer Coupling, *Adv. Mater.*, 2013, **25**, 899.
- 116 K. Kaasbjerg, K. S. Thygesen and K. W. Jacobsen, Phonon-limited mobility in n-type single-layer MoS₂ from first principles, *Phys. Rev. B: Condens. Matter Mater. Phys.*, 2012, **85**, 115317.
- 117 K. Kaasbjerg, K. S. Thygesen and A.-P. Jauho, Acoustic phonon limited mobility in two-dimensional semiconductors: Deformation potential and piezoelectric scattering in monolayer MoS₂ from first principles, *Phys. Rev. B: Condens. Matter Mater. Phys.*, 2013, **87**, 235312.
- 118 D. Jariwala, V. K. Sangwan, D. J. Late, J. E. Johns, V. P. Dravid, T. J. Marks, L. J. Lauhon and M. C. Hersam, Band-like transport in high mobility unencapsulated single-layer MoS₂ transistors, *Appl. Phys. Lett.*, 2013, **102**, 173107.
- 119 J. Wu, H. Schmidt, K. K. Amara, X. Xu, G. Eda and B. Özyilmaz, Large Thermoelectricity via Variable Range Hopping in Chemical Vapor Deposition Grown Single-Layer MoS₂, *Nano Lett.*, 2014, **14**, 2730.
- 120 N. Petrone, C. R. Dean, I. Meric, A. M. van der Zande, P. Y. Huang, L. Wang, D. Muller, K. L. Shepard and J. Hone, Chemical Vapor Deposition-Derived Graphene with Electrical Performance of Exfoliated Graphene, *Nano Lett.*, 2012, **12**, 2751.
- 121 S.-L. Li, K. Wakabayashi, Y. Xu, S. Nakaharai, K. Komatsu, W.-W. Li, Y.-F. Lin, A. Aparecido-Ferreira and K. Tsukagoshi, Thickness-Dependent Interfacial Coulomb Scattering in Atomically Thin Field-Effect Transistors, *Nano Lett.*, 2013, **13**, 3546.
- 122 W. Bao, X. Cai, D. Kim, K. Sridhara and M. S. Fuhrer, High mobility ambipolar MoS₂ field-effect transistors: Substrate and dielectric effects, *Appl. Phys. Lett.*, 2013, **102**, 042104.
- 123 G.-H. Lee, Y.-J. Yu, X. Cui, N. Petrone, C.-H. Lee, M. S. Choi, D.-Y. Lee, C. Lee, W. J. Yoo, K. Watanabe, T. Taniguchi, C. Nuckolls, P. Kim and J. Hone, Flexible and Transparent MoS₂ Field-Effect Transistors on Hexagonal Boron Nitride-Graphene Heterostructures, *ACS Nano*, 2013, **7**, 7931.

- 124 E. S. Kadantsev and P. Hawrylak, Electronic structure of a single MoS₂ monolayer, *Solid State Commun.*, 2012, **152**, 909.
- 125 B. Chamlagain, Q. Li, N. J. Ghimire, H.-J. Chuang, M. M. Perera, H. Tu, Y. Xu, M. Pan, D. Xaio, J. Yan, D. Mandrus and Z. Zhou, Mobility Improvement and Temperature Dependence in MoSe₂ Field-Effect Transistors on Parylene-C Substrate, *ACS Nano*, 2014, **8**, 5079.
- 126 J. Qiao, X. Kong, Z.-X. Hu, F. Yang and W. Ji, High-mobility transport anisotropy and linear dichroism in few-layer black phosphorus, *Nat. Commun.*, 2014, **5**, 4475.
- 127 M. Y. Chan, K. Komatsu, S.-L. Li, Y. Xu, P. Darmawan, H. Kuramochi, S. Nakaharai, A. Aparecido-Ferreira, K. Watanabe, T. Taniguchi and K. Tsukagoshi, Suppression of thermally activated carrier transport in atomically thin MoS₂ on crystalline hexagonal boron nitride substrates, *Nanoscale*, 2013, **5**, 9572.
- 128 S. Das, H.-Y. Chen, A. V. Penumatcha and J. Appenzeller, High Performance Multilayer MoS₂ Transistors with Scandium Contacts, *Nano Lett.*, 2013, **13**, 100.
- 129 J.-H. Chen, C. Jang, S. Adam, M. S. Fuhrer, E. D. Williams and M. Ishigami, Charged-impurity scattering in graphene, *Nat. Phys.*, 2008, **4**, 377.
- 130 J.-H. Chen, C. Jang, S. Xiao, M. Ishigami and M. S. Fuhrer, Intrinsic and extrinsic performance limits of graphene devices on SiO₂, *Nat. Nanotechnol.*, 2008, **3**, 206.
- 131 C. R. Dean, A. F. Young, I. Meric, C. Lee, L. Wang, S. Sorgenfrei, K. Watanabe, T. Taniguchi, P. Kim, K. L. Shepard and J. Hone, Boron nitride substrates for high-quality graphene electronics, *Nat. Nanotechnol.*, 2010, **5**, 722.
- 132 N. Ma and D. Jena, Charge Scattering and Mobility in Atomically Thin Semiconductors, *Phys. Rev. X*, 2014, **4**, 011043.
- 133 D. J. Late, B. Liu, H. S. S. R. Matte, V. P. Dravid and C. N. R. Rao, Hysteresis in Single-Layer MoS₂ Field Effect Transistors, *ACS Nano*, 2012, **6**, 5635.
- 134 J.-R. Chen, P. M. Odenthal, A. G. Swartz, G. C. Floyd, H. Wen, K. Y. Luo and R. K. Kawakami, Control of Schottky Barriers in Single Layer MoS₂ Transistors with Ferromagnetic Contacts, *Nano Lett.*, 2013, **13**, 3106.
- 135 Y. Guo, Y. Han, J. Li, A. Xiang, X. Wei, S. Gao and Q. Chen, Study on the Resistance Distribution at the Contact between Molybdenum Disulfide and Metals, *ACS Nano*, 2014, **8**, 7771.
- 136 W. Liu, J. Kang, D. Sarkar, Y. Khatami, D. Jena and K. Banerjee, Role of Metal Contacts in Designing High-Performance Monolayer n-Type WSe₂ Field Effect Transistors, *Nano Lett.*, 2013, **13**, 1983.
- 137 C. Gong, L. Colombo, R. M. Wallace and K. Cho, The Unusual Mechanism of Partial Fermi Level Pinning at Metal–MoS₂ Interfaces, *Nano Lett.*, 2013, **14**, 1714.
- 138 S. M. Sze and K. K. Ng, *Physics of Semiconductor Devices*, John Wiley & Sons, Inc., 2007.
- 139 D. Kiriya, M. Tosun, P. Zhao, J. S. Kang, J. Seuk and A. Javey, Air-Stable Surface Charge Transfer Doping of MoS₂ by Benzyl Viologen, *J. Am. Chem. Soc.*, 2014, **136**, 7853.
- 140 S. Mouri, Y. Miyauchi and K. Matsuda, Tunable Photoluminescence of Monolayer MoS₂ via Chemical Doping, *Nano Lett.*, 2013, **13**, 5944.
- 141 J. S. Oh, K. N. Kim and G. Y. Yeom, Graphene Doping Methods and Device Applications, *J. Nanosci. Nanotechnol.*, 2014, **14**, 1120.
- 142 H. Y. Mao, Y. H. Lu, J. D. Lin, S. Zhong, A. T. S. Wee and W. Chen, Manipulating the electronic and chemical properties of graphene via molecular functionalization, *Prog. Surf. Sci.*, 2013, **88**, 132.
- 143 M. Batzill, The surface science of graphene: Metal interfaces, CVD synthesis, nanoribbons, chemical modifications, and defects, *Surf. Sci. Rep.*, 2012, **67**, 83.
- 144 D. Liming, Functionalization of Graphene for Efficient Energy Conversion and Storage, *Acc. Chem. Res.*, 2013, **46**, 31.
- 145 D. Zhan, J. Yan, L. Lai, Z. Ni, L. Liu and Z. Shen, Engineering the Electronic Structure of Graphene, *Adv. Mater.*, 2012, **24**, 4055.
- 146 R. S. Lee, H. J. Kim, J. E. Fischer, J. Lefebvre, M. Radosavljević, J. Hone and A. T. Johnson, Transport properties of a potassium-doped single-wall carbon nanotube rope, *Phys. Rev. B: Condens. Matter Mater. Phys.*, 2000, **61**, 4526.
- 147 V. Sgobba and D. M. Guldi, Carbon nanotubes—electronic/electrochemical properties and application for nanoelectronics and photonics, *Chem. Soc. Rev.*, 2008, **38**, 165.
- 148 J. E. Fischer, Chemical Doping of Single-Wall Carbon Nanotubes, *Acc. Chem. Res.*, 2002, **35**, 1079.
- 149 R. H. Fried and A. D. Yoffe, Electronic properties of intercalation complexes of the transition metal dichalcogenides, *Adv. Phys.*, 1987, **36**, 1.
- 150 F. K. Perkins, A. L. Friedman, E. Cobas, P. M. Campbell, G. G. Jernigan and B. T. Jonker, Chemical Vapor Sensing with Monolayer MoS₂, *Nano Lett.*, 2013, **13**, 668.
- 151 Y. Du, H. Liu, A. T. Neal, M. Si and P. D. Ye, Molecular Doping of Multilayer MoS₂ Field-Effect Transistors: Reduction in Sheet and Contact Resistances, *IEEE Electron Device Lett.*, 2013, **34**, 1328.
- 152 S. Dey, H. S. S. R. Matte, S. N. Shirodkar, U. V. Waghmare and C. N. R. Rao, Charge-Transfer Interaction between Few-Layer MoS₂ and Tetrathiafulvalene, *Chem. – Asian J.*, 2013, **8**, 1780.
- 153 S. Tongay, J. Zhou, C. Ataca, J. Liu, J. S. Kang, T. S. Matthews, L. You, J. Li, J. C. Grossman and J. Wu, Broad-Range Modulation of Light Emission in Two-Dimensional Semiconductors by Molecular Physisorption Gating, *Nano Lett.*, 2013, **13**, 2831.
- 154 H. Nan, Z. Wang, W. Wang, Z. Liang, Y. Lu, Q. Chen, D. He, P. Tan, F. Miao, W. Feng, X. Wang, J. Wang and Z. Ni, Strong Photoluminescence Enhancement of MoS₂ through Defect Engineering and Oxygen Bonding, *ACS Nano*, 2014, **8**, 5738.
- 155 Y. Shi, J.-K. Huang, L. Jin, Y.-T. Hsu, S. F. Yu, L.-J. Li and H. Y. Yang, Selective Decoration of Au Nanoparticles on Monolayer MoS₂ Single Crystals, *Sci. Rep.*, 2013, **3**, 1839.

- 156 J. Lin, J. Zhong, S. Zhong, H. Li, H. Zhang and W. Chen, Modulating electronic transport properties of MoS₂ field effect transistor by surface overlayers, *Appl. Phys. Lett.*, 2013, **103**, 063109.
- 157 K. Chen, D. Kiriya, M. Hettick, M. Tosun, T.-J. Ha, S. R. Madhvapathy, S. Desai, A. Sachid and A. Javey, Air stable n-doping of WSe₂ by silicon nitride thin films with tunable fixed charge density, *APL Mater.*, 2014, **2**, 092504.
- 158 J. D. Lin, C. Han, F. Wang, R. Wang, D. Xiang, S. Qin, X.-A. Zhang, L. Wang, H. Zhang, A. T. S. Wee and W. Chen, Electron-Doping-Enhanced Trion Formation in Monolayer Molybdenum Disulfide Functionalized with Cesium Carbonate, *ACS Nano*, 2014, **8**, 5323.
- 159 H. Fang, M. Tosun, G. Seol, T. C. Chang, K. Takei, J. Guo and A. Javey, Degenerate n-Doping of Few-Layer Transition Metal Dichalcogenides by Potassium, *Nano Lett.*, 2013, **13**, 1991.
- 160 S. Chuang, C. Battaglia, A. Azcatl, S. McDonnell, J. S. Kang, X. Yin, M. Tosun, R. Kapadia, H. Fang, R. M. Wallace and A. Javey, MoS₂ P-type Transistors and Diodes Enabled by High Work Function MoO_x Contacts, *Nano Lett.*, 2014, **14**, 1337.
- 161 Y. Du, L. Yan, H. Liu and P. D. Ye, Contact research strategy for emerging molybdenum disulfide and other two-dimensional field-effect transistors, *APL Mater.*, 2014, **2**, 092510.
- 162 H. Qiu, L. Pan, Z. Yao, J. Li, Y. Shi and X. Wang, Electrical characterization of back-gated bi-layer MoS₂ field-effect transistors and the effect of ambient on their performances, *Appl. Phys. Lett.*, 2012, **100**, 123104.
- 163 D. W. Murphy, F. J. Di Salvo, G. W. Hull and J. V. Waszczak, Convenient Preparation and Physical Properties of Lithium Intercalation Compounds of Group 4B and 5B Layered Transition Metal Dichalcogenides, *Inorg. Chem.*, 1976, **15**, 17.
- 164 R. B. Somoano and A. Rembaum, Superconductivity in Intercalated Molybdenum Disulfide, *Phys. Rev. Lett.*, 1971, **27**, 402.
- 165 M. B. Dines, Lithium intercalation via n-butyllithium of the layered Transition metal dichalcogenides, *Mater. Res. Bull.*, 1975, **10**, 287.
- 166 H.-L. Tsai, J. Heising, J. L. Schindler, C. R. Kannewurf and M. G. Kanatzidis, Exfoliated-Restacked Phase of WS₂, *Chem. Mater.*, 1997, **9**, 879.
- 167 S. Wu, Z. Zeng, Q. He, Z. Wang, S. J. Wang, Y. Du, Z. Yin, X. Sun, W. Chen and H. Zhang, Electrochemically Reduced Single-Layer MoS₂, *Small*, 2012, **8**, 2264.
- 168 M. A. Py and R. R. Haering, Structural destabilization induced by lithium intercalation in MoS₂ and related compounds, *Can. J. Phys.*, 1983, **61**, 76.
- 169 G. Eda, H. Yamaguchi, D. Voiry, T. Fujita, M. Chen and M. Chhowalla, Photoluminescence from Chemically Exfoliated MoS₂, *Nano Lett.*, 2011, **11**, 5111.
- 170 H. Wang, Z. Lu, S. Xu, D. Kong, J. J. Cha, G. Zheng, P.-C. Hsu, K. Yan, D. Bradshaw, F. B. Prinz and Y. Cui, Electrochemical tuning of vertically aligned MoS₂ nanofilms and its application in improving hydrogen evolution reaction, *Proc. Natl. Acad. Sci. U. S. A.*, 2013, **110**, 19701.
- 171 L. Wang, Z. Xu, W. Wang and X. Bai, Atomic Mechanism of Dynamic Electrochemical Lithiation Processes of MoS₂ Nanosheets, *J. Am. Chem. Soc.*, 2014, **136**, 6693.
- 172 H. Wang, Z. Lu, D. Kong, J. Sun, T. M. Hymel and Y. Cui, Electrochemical Tuning of MoS₂ Nanoparticles on Three-Dimensional Substrate for Efficient Hydrogen Evolution, *ACS Nano*, 2014, **8**, 4940.
- 173 C. A. Papageorgopoulos and W. Jaegermann, Li intercalation across and along the van der Waals and surfaces and of MO and (0001), *Surf. Sci.*, 1995, **338**, 83.
- 174 D. Voiry, M. Salehi, R. Silva, T. Fujita, M. Chen, T. Asefa, V. B. Shenoy, G. Eda and M. Chhowalla, Conducting MoS₂ Nanosheets as Catalysts for Hydrogen Evolution Reaction, *Nano Lett.*, 2013, **13**, 6222.
- 175 Y.-C. Lin, D. O. Dumcenco, Y.-S. Huang and K. Suenaga, Atomic mechanism of the semiconducting-to-metallic phase transition in single-layered MoS₂, *Nat. Nanotechnol.*, 2014, **9**, 391.
- 176 R. Kappera, D. Voiry, S. E. Yalcin, B. Branch, G. Gupta, A. D. Mohite and M. Chhowalla, Phase-engineered low-resistance contacts for ultrathin MoS₂ transistors, *Nat. Mater.*, 2014, 4080.
- 177 A. Ulman, Formation and Structure of Self-Assembled Monolayers, *Chem. Rev.*, 1996, **96**, 1533.
- 178 N. Cernetichan, S. Wu, J. A. Davies, B. W. Krueger, D. O. Hutchins, X. Xu, H. Ma and A. K.-Y. Jen, Systematic Doping Control of CVD Graphene Transistors with Functionalized Aromatic Self-Assembled Monolayers, *Adv. Funct. Mater.*, 2014, **24**, 3464.
- 179 H. Lv, H. Wu, K. Xiao, W. Zhu, H. Xu, Z. Zhang and H. Qian, Graphene mobility enhancement by organo-silane interface engineering, *Appl. Phys. Lett.*, 2013, **102**, 183107.
- 180 Y. Li, C.-Y. Xu, P. Hu and L. Zhen, Carrier Control of MoS₂ Nanoflakes by Functional Self-Assembled Monolayers, *ACS Nano*, 2013, **7**, 7795.
- 181 T. Moehl, M. A. E. Halim and H. Tributsch, Photoelectrochemical studies on the n-MoS₂-Cysteine interaction, *J. Appl. Electrochem.*, 2006, **36**, 1341.
- 182 L. Cheng, X. Qin, A. T. Lucero, A. Azcatl, J. Huang, R. M. Wallace, K. Cho and J. Kim, Atomic Layer Deposition of a High-k Dielectric on MoS₂ Using Trimethylaluminum and Ozone, *ACS Appl. Mater. Interfaces*, 2014, **6**, 11834.
- 183 C. Haensch, S. Hoeppener and U. S. Schubert, Chemical modification of self-assembled silane based monolayers by surface reactions, *Chem. Soc. Rev.*, 2010, **39**, 2323.
- 184 E. L. Hanson, J. Schwartz, B. Nickel, N. Koch and M. F. Danisman, Bonding Self-Assembled, Compact Organophosphonate Monolayers to the Native Oxide Surface of Silicon, *J. Am. Chem. Soc.*, 2003, **125**, 16074.
- 185 K. S. Midwood, M. D. Carolus, M. P. Danahy, J. E. Schwarzbauer and J. Schwartz, Easy and Efficient Bonding of Biomolecules to an Oxide Surface of Silicon, *Langmuir*, 2004, **20**, 5501.

- 186 M. Dubey, T. Weidner, L. J. Gamble and D. G. Castner, Structure and Order of Phosphonic Acid-Based Self-Assembled Monolayers on Si(100), *Langmuir*, 2010, **26**, 14747.
- 187 S. W. Wu, G. V. Nazin, X. Chen, X. H. Qiu and W. Ho, Control of Relative Tunneling Rates in Single Molecule Bipolar Electron Transport, *Phys. Rev. Lett.*, 2004, **93**, 236802.
- 188 A. Kay and M. Graetzel, Dye-Sensitized Core-Shell Nanocrystals: Improved Efficiency of Mesoporous Tin Oxide Electrodes Coated with a Thin Layer of an Insulating Oxide, *Chem. Mater.*, 2002, **14**, 2930.
- 189 O. Pirrotta, L. Larcher, M. Lanza, A. Padovani, M. Porti, M. Nafría and G. Bersuker, Leakage current through the poly-crystalline HfO₂: Trap densities at grains and grain boundaries, *J. Appl. Phys.*, 2013, **114**, 134503.
- 190 R. M. C. de Almeida and I. J. R. Baumvol, Reaction-diffusion in high-k dielectrics on Si, *Surf. Sci. Rep.*, 2003, **49**, 1.
- 191 T. E. Hartman and J. S. Chivian, Electron Tunneling Through Thin Aluminum Oxide Films, *Phys. Rev.*, 1964, **134**, A1094.
- 192 L. Giordano and G. Pacchioni, Oxide Films at the Nano-scale: New Structures, New Functions, and New Materials, *Acc. Chem. Res.*, 2011, **44**, 1244.
- 193 A. Ghorbal, F. Grisotto, M. Laude, J. Charlier and S. Palacin, The *in situ* characterization and structuring of electrografted polyphenylene films on silicon surfaces. An AFM and XPS study, *J. Colloid Interface Sci.*, 2008, **328**, 308.
- 194 J.-Y. Lee, J. G. Lee, S.-H. Lee, M. Seo, L. Piao, J. H. Bae, S. Y. Lim, Y. J. Park and T. D. Chung, Hydrogen-atom-mediated electrochemistry, *Nat. Commun.*, 2013, **4**, 2766.
- 195 Y. Liu, E. Kim, R. V. Ulijn, W. E. Bentley and G. F. Payne, Reversible Electroaddressing of Self-assembling Amino-Acid Conjugates, *Adv. Funct. Mater.*, 2011, **21**, 1575.
- 196 Y. Liu, Y. Cheng, H.-C. Wu, E. Kim, R. V. Ulijn, G. W. Rubloff, W. E. Bentley and G. F. Payne, Electroaddressing Agarose Using Fmoc-Phenylalanine as a Temporary Scaffold, *Langmuir*, 2011, **27**, 7380.
- 197 D. Belanger and J. Pinson, Electrografting: a powerful method for surface modification, *Chem. Soc. Rev.*, 2011, **40**, 3995.
- 198 S. Mahouche-Chergui, S. Gam-Derouich, C. Mangeney and M. M. Chehimi, Aryl diazonium salts: a new class of coupling agents for bonding polymers, biomacromolecules and nanoparticles to surfaces, *Chem. Soc. Rev.*, 2011, **40**, 4143.
- 199 N. K. Devaraj, P. H. Dinolfo, C. E. D. Chidsey and J. P. Collman, Selective Functionalization of Independently Addressed Microelectrodes by Electrochemical Activation and Deactivation of a Coupling Catalyst, *J. Am. Chem. Soc.*, 2006, **128**, 1794.
- 200 T. S. Hansen, A. E. Daugaard, S. Hvilsted and N. B. Larsen, Spatially Selective Functionalization of Conducting Polymers by Electroclick Chemistry, *Adv. Mater.*, 2009, **21**, 4483.
- 201 X.-W. Shi, X. Yang, K. J. Gaskell, Y. Liu, E. Kobatake, W. E. Bentley and G. F. Payne, Reagentless Protein Assembly Triggered by Localized Electrical Signals, *Adv. Mater.*, 2009, **21**, 984.
- 202 Y. Wang, T. Wang, P. Da, M. Xu, H. Wu and G. Zheng, Silicon Nanowires for Biosensing, Energy Storage, and Conversion, *Adv. Mater.*, 2013, **25**, 5177.
- 203 F. Patolsky, G. Zheng and C. M. Lieber, Nanowire sensors for medicine and the life science, *Future Medicine*, 2006, **1**, 51.
- 204 H. K. Hunt and A. M. Armani, Label-free biological and chemical sensors, *Nanoscale*, 2010, **2**, 1544.
- 205 S. Roy and Z. Gao, Nanostructure-based electrical biosensors, *Nano Today*, 2009, **4**, 318.
- 206 P. M. Mendes, Stimuli-responsive surfaces for bio-applications, *Chem. Soc. Rev.*, 2008, **11**, 2361.
- 207 I. S. Choi and Y. S. Chi, Surface Reactions On Demand: Electrochemical Control of SAM-Based Reactions, *Angew. Chem., Int. Ed.*, 2006, **45**, 4894.
- 208 P. Vanýsek, Electrochemical Series, *Handbook of Chemistry and Physics*, Chemical Rubber Company, 92nd edn, 2011.
- 209 C. M. A. Brett and M. O. Brett, *Electrochemistry Principles, Methods and Applications*, Oxford University Press Inc, New York City, 1993.
- 210 M. S. Ram and D. M. Stanbury, *Inorg. Chem.*, 1985, **24**, 2954.
- 211 P. Atkins, *Physical Chemistry*, W. H. Freeman and Company, New York City, 6th edn, 1997.
- 212 X. Cui, G.-H. Lee, Y. D. Kim, G. Arefe, P. Y. Huang, C.-H. Lee, D. A. Chenet, X. Zhang, L. Wang, F. Ye, F. Pizzocchero, B. S. Jessen, K. Watanabe, T. Taniguchi, D. A. Muller, T. Low, P. Kim and J. Hone, Multi-terminal transport measurements of MoS₂ using a van der Waals heterostructure device platform, *Nat. Nanotechnol.*, 2015, **10**, 534.